

Validation of a novel subject-specific musculoskeletal strength-scaling workflow using submaximal dynamic strength tests

Bjørn Keller Jensen, Cecilie Bjørn Jensen, and Mads Kattrup Pedersen
Sports Technology, 19gr10201, June 2019

Master's Thesis





Department of Health Science and Technology
Aalborg University
www.hst.aau.dk

AALBORG UNIVERSITY

STUDENT REPORT

Title:

Validation of a novel subject-specific musculoskeletal strength-scaling workflow using submaximal dynamic strength tests

Theme:

Master's Thesis

Project Period:

Spring semester 2019

Project Group:

19gr10201

Participants:

Bjørn Keller Jensen
Cecilie Bjørn Jensen
Mads Kattrup Pedersen

Supervisors:

Mark de Zee
John Rasmussen

Pages: 49

Date of Completion:

6th of June 2019

Abstract:

Introduction: The present study aimed at creating and verifying a workflow to perform subject-specific strength-scaling of musculoskeletal models, and validating the strength-scaled models using isometric joint torque measurements. **Methods:** The participants consisted of 21 males and 7 females. A field strength assessment across 10 exercises was used to estimate the participants' one-repetition-maximum (1RM). The 1RM measures were implemented in an optimization routine, calculating a set of strength factors capable of scaling all included muscles in the 10 different exercise-specific musculoskeletal models. Further, peak joint torques were investigated using dynamometer obtained isometric strength measurements for elbow flexion and extension, knee flexion and extension, and ankle plantar flexion. **Results:** The optimization based strength-scaled models showed an improvement of mean normalized root mean square error from 48.39 (± 22.99) % to 28.13 (± 15.47) % compared to the standard-scaled models. **Discussion:** The optimization routine was faster than previously used methods and showed a higher accuracy than the standard strength-scaling of musculoskeletal models. Issues in the simple muscle models wrapping around the knee and ankle joints made the comparison with the dynamometer data infeasible. The present study shows an improvement when applying the optimization routine for whole body musculoskeletal models, and other or more exercises could easily be implemented for scalability. However, utilizing simple musculoskeletal muscle models cannot readily be used to estimate and compare peak joint torque for near end range of motion angles.

Validation of a novel subject-specific musculoskeletal strength-scaling workflow using submaximal dynamic strength tests

Bjørn Keller Jensen¹, Cecilie Bjørn Jensen¹, and Mads Kattrup Pedersen¹

¹*Department of Health Science and Technology, Aalborg University, Denmark*

Handed in: 6th of June 2019

Abstract

Introduction: The present study aimed at creating and verifying a workflow to perform subject-specific strength-scaling of musculoskeletal models, and validating the strength-scaled models using isometric joint torque measurements. **Methods:** The participants consisted of 21 males and 7 females. A field strength assessment across 10 exercises was used to estimate the participants' one-repetition-maximum (1RM). The 1RM measures were implemented in an optimization routine, calculating a set of strength factors capable of scaling all included muscles in the 10 different exercise-specific musculoskeletal models. Further, peak joint torques were investigated using dynamometer obtained isometric strength measurements for elbow flexion and extension, knee flexion and extension, and ankle plantar flexion. **Results:** The optimization based strength-scaled models showed an improvement of mean normalized root mean square error from 48.39 (± 22.99) % to 28.13 (± 15.47) % compared to the standard-scaled models. **Discussion:** The optimization routine was faster than previously used methods and showed a higher accuracy than the standard strength-scaling of musculoskeletal models. Issues in the simple muscle models wrapping around the knee and ankle joints made the comparison with the dynamometer data infeasible. The present study shows an improvement when applying the optimization routine for whole body musculoskeletal models, and other or more exercises could easily be implemented for scalability. However, utilizing simple musculoskeletal muscle models cannot readily be used to estimate and compare peak joint torque for near end range of motion angles.

Keywords: *Musculoskeletal model validation, Musculoskeletal scaling, AnyBody Modeling System, Strength Exercise, One-repetition-maximum estimation, Mathematical optimization, Isometric strength, Strength-scaling.*

Introduction

A paradigm shift from creating standard musculoskeletal models to subject-specific scaled models has evolved extensively over the last decade. Complex techniques for obtaining subject-specific anthropometric and geometric input data such as; bone surfaces [1], tendon properties [2], and musculoskeletal geometry [3] have made it possible to accurately scale cadaver-based musculoskeletal models to represent specific subjects.

Parallel to the developments in anthropometric scaling, the strength-scaling (SS) of musculoskeletal models, especially when creating subject-specific models, has not undergone the same develop-

ment. Accurate subject-specific estimations of internal forces have long been sought as the next step in musculoskeletal modeling [4] and could aid in designing prosthetics, surgical planning and refining strategies for athlete training schemes. Common for all scaling methods should be their ability to scale the mass, geometry and strength properties of the underlying cadaver models used in musculoskeletal software [5, 6]. Currently, commercial musculoskeletal modeling software, such as the AnyBody Modeling System (AMS), provides different standard scaling laws suitable for different types of models [7]. A general method is the *uniform scaling law*, which scales the geometry equally in all three dimensions, while scaling the muscle strengths to a non-linear power of $\frac{2}{3}$. A more ad-

vanced and subject-specific method is the *XYZ scaling law* which allow the modeler to input scaling factors derived from anthropometric databases, to create models representing percentiles of populations or specific subjects. The strength scales accordingly to the *Length-Mass-Fat (LMF) scaling law* [7], which have been widely implemented [8–10] and incorporates the estimated fat percentage of the subject to ensure that short subjects with high masses do not necessarily have more force producing capacity [7]. Common for the current SS methods are their inability to encapsulate subject-specific strength variations between two anthropometrically equal subjects.

Previous studies have tried to bridge the gap between experimentally obtained maximum strength measures and musculoskeletal model strength, aimed at more subject specificity [11–13]. D’Souza et al. [11] developed a multiple linear regression formula, using anthropometric predictors, to estimate peak joint torque (PJT). Such regression equations could readily be implemented in a musculoskeletal model to improve the SS. Oomen et al. [12] developed a rule-based SS method and validated it against different standard methods including the LMF method. Their results indicated that the LMF method significantly underestimated the lower-extremity strength, while the standard strength of the TLEM 1.0 dataset [14] and their rule-based SS method resulted in better strength estimations. Concludingly, they argued that care should be taken when applying the current SS methods in subject-specific models.

Heinen et al. [13] implemented a two-step optimization routine using subject-specific isometric and iso-velocity torque profiles to scale the muscle tendon parameters needed in a 3-element Hill-type (3E) muscle model [15]. They found that the isometric torque data provided the largest decrease in normalized root mean square values. However, adding an iso-velocity optimization did not improve the results to an extent where the extra strain on the subjects and the cumbersome data collection was worth the gain in accuracy [13]. Although they did not report the computational time of their optimization routines, performing an inverse dynamics analysis over a dynamic movement with multiple timesteps and design variables, it is unlikely that it is practically applicable, even when only including the lower extremity model. The Hill-type muscle model forms a good phenomenological representation of muscle contraction dynamics, however, obtaining the parameters needed for its calibration can be a difficult task [16]. Instead, researchers

have successfully utilized a simple muscle model without force-length or force-velocity profiles for investigating knee joint contact forces [17, 18], spinal loads [19], and glenohumeral stability as a consequence of rotator cuff tears [20].

When working with muscle force estimations, the muscle load sharing redundancy has been resolved by optimization schemes, to form different criteria capable of representing the complex underlying physiology. Obtaining subject-specific muscle strength estimations could help the muscle recruitment criterion, in terms of limiting the maximum force output of the muscle models to physiologically realistic values, thereby acting as a boundary condition [4, 21].

To summarize, implementing regression formulas seems to be infeasible in subject-specific SS. Additionally, using complex muscle models and strength parameters, such as isometric or iso-velocity measurements that are difficult to obtain, further complicates the process of SS. Hence, identifying easy-to-measure parameters, describing the force capabilities of skeletal muscles, combined with mathematical optimization routines could be utilized to create reliable and practical SS of subject-specific musculoskeletal muscle models. These maximum strength parameters should preferably be obtained without expensive machines, such as dynamometers, while the optimization routine should be fast enough to be practically applicable.

Examining the strength exercise literature, a practical and reliable method of obtaining maximum strength assessments is the use of one-repetition-maximum (1RM) measures [22]. A 1RM is defined as the maximum mass that an individual is able to move through a given range of motion (ROM). Although the measure is easy to understand, it can be tedious to obtain, as it imposes a relatively high risk of repetition failure and injury when the intensity of the exercise increases. Several researchers have sought easier methods to obtain 1RM estimates. These include the use of regression formulas to estimate 1RM, based on submaximal repetitions until fatigue [22, 23]. An abundance of algorithms have been developed and presented throughout the literature, showing good results on varying populations and exercises [22, 24–26].

When altering previously validated musculoskeletal models and implementing subject-specific scaling, it is wise to ensure that the imposed scaling does not alter the model to a degree where it is no longer representative of the physiological systems that they simulate [27]. It is important to consider possible verifica-

tion and validation schemes in order to ensure reliable models. Such schemes could be validating a method using a dataset not used to develop the method, as implemented by Oomen et al. [12].

To the best of our knowledge, no method exists to input simple anthropometric measures, $1RM$ estimations and static optimization in order to perform subject-specific SS of simple musculoskeletal muscle models. Therefore, the present study aimed at 1) creating and verifying a workflow to perform subject-specific SS of musculoskeletal models, and 2) validating the strength scaled-models using isometric joint torque measurements.

Methods

Experimental design

The experimental design consisted of two parts. The first part focused on verification of the methodology regarding subject-specific SS of musculoskeletal models based on dynamic strength measurements. This involved a field test session for each participant, testing their individual 3-7 repetition-maximum in 10 different exercises, consisting of seven upper and three lower body exercises. The second part focused on validating the optimization based strength-scaled models by testing the participants' isometric strength, using a dynamometer.

Part 1

The verification experiment consisted of a field test at a local fitness center, testing each participant's dynamic submaximal strength in 10 different strength exercises, focusing on most major muscle groups. Unilateral exercises were performed using the right side of the body and consisted of; biceps curl, calf raise, lateral pulldown, lateral raise, leg curl, leg extension, side bends, and triceps extension. Whereas the bench press and horizontal row, were performed as bilateral exercises due to their technical requirement.

Subjects

28 healthy participants were recruited and consisted of 21 males and 7 females. The participants had a mean (\pm SD) age of 28.11 (\pm 7.68) years, stature of 1.81 (\pm 0.08) m and body mass of 90.2 (\pm 19.02) kg. No participants had suffered injuries within the last three months prior to testing. The participants answered a series of questions regarding their physical activity levels, weekly participation in sports, and experience with strength exercise. The participants showed a wide range of experience with strength train-

ing, from novice (first time in a fitness center) to expert (national powerlifting team member). The study was conducted in accordance with the guidelines set through the Declaration of Helsinki, with all participants giving their written consent before participating.

Protocol

The field test session began with noting 15 anthropometric measures of the participant. Subsequently, a 15-minute dynamic mobility warm-up routine was completed, specifically targeting all major muscle groups. Furthermore, before each exercise, the participant would perform an exercise-specific warm-up, consisting of 1-2 sets with an increasing load immediately before the test sets. The specific warm-up acted both as a familiarization of the required technique for the exercise, and as a warm-up of the targeted muscles. For both the specific warm-up and test sets, the test-leader and the participant agreed upon the inter-set mass increments. The goal for the test sets was to increase the load rapidly to limit the number of sets performed, and thereby minimize fatigue. After the specific warm-up, a one-minute rest period was given before the participant started the test set. The goal was to complete one set with a mass that the participant was only able to perform 3-7 repetitions with. If the participant completed eight repetitions, the set was terminated and the mass was incremented for another set. Each test set was separated by a one-minute rest period, and a two-minute rest period separated the exercises. The order of exercises was chosen to ensure that the same muscle groups were not tested on two consecutive exercises (e.g. the horizontal row could not follow the lateral pulldown and vice versa).

To ensure the applied mass of each exercise machine was noted correctly, the gearings of the machines were measured using a handheld analogue ring dynamometer (Tiedemann Instruments GmbH & Co. KG, Garmisch-Partenkirchen, Germany). The labeled loads on the strength exercise machines were plotted against the values from the ring dynamometer, after a conversion from μm to kg, and a linear relationship was found ($R^2 > 0.95$). Therefore, participant's recorded mass moved was multiplied by the regression coefficient from the linear regression equation found for each strength exercise machine. This was done for the biceps curl, horizontal row, lateral pulldown, leg curl, leg extension, and triceps extension exercises.

Estimating 1RM

The Wathan regression formula [23, 28] (equation 1) was selected to estimate 1RM based on the mass moved and the number of completed repetitions during the last set, due to its performance in multiple strength exercises resembling the included exercises.

$$1RM = \frac{100m}{48.8 + 53.8e^{-0.075n_{reps}}} \quad (1)$$

where m is the mass [kg] moved and n_{reps} is the number of repetitions performed. The estimated 1RM served as a measure of subject-specific dynamic strength for each exercise and was used in the optimization workflow.

Musculoskeletal exercise models

To model all exercises as computer-based musculoskeletal models, the AnyBody Modeling System (AMS) ver. 7.2 beta (AnyBody Technology A/S, Aalborg, Denmark) was used [6]. All models were based on the human model template in the AnyBody Managed Model Repository (AMMR) ver. 2.2.0 [29]. Each model included the TLEM 2.0 leg model [3], detailed neck model [30], lumbar spine model [31], and the shoulder-arm model [32]. Each model included a total of 918 muscle actuators, which were modeled as simple muscle models with only a nominal strength parameter, and no force-velocity or force-length relationships were taken into account. For all models the min/max muscle recruitment criterion was used [21]. A quadratic auxiliary term of 0.0001 was added to stabilize the inverse dynamics solution. All models were kinematically overdeterminate, which was solved through the AMS overdeterminate solver [33]. This involved deciding which constraints the solver was able to treat as *soft* and should be fulfilled "as good as possible", and which constraints were *hard* and could not be violated, based on how the exercise was performed in the fitness center. Furthermore, to control the exercise movement, the *WeakDriverWeight* was altered for certain drivers, in order to control the movement and mimic the strength exercises.

Geometrical scaling

In order to geometrically scale each model to represent the participants' anthropometrics, the *XYZ scaling law* was implemented. The law scales each segment linearly as defined by Rasmussen et al. [7]:

$$s = \mathbf{S}p + t \quad (2)$$

where s represents the scaled node's position vector in

its local coordinate system, p is the positional vector of the unscaled node, and t represents a translational vector of the segment's local coordinate system on the scaled segment. \mathbf{S} is a 3×3 diagonal scaling matrix, given by:

$$\mathbf{S} = \begin{bmatrix} k_x & & \\ & k_y & \\ & & k_z \end{bmatrix} \quad (3)$$

where k is the scaling factor, which are calculated based on subject-specific anthropometric data, measured in accordance with the ANSUR dataset [34]. A kinematic optimization study [35] was applied to a standard AMS model, resulting in subject-specific scaling factors for each of the ANSUR subjects. Using the ANSUR anthropometric measures and corresponding scaling factors as a basic population, and setting the measured participants' anthropometrics as primal constraints, a closed-form optimization problem utilizing a PCA resulted in subject-specific scaling factors for each participant.

Initial strength-scaling

The initial muscle strength (f) is calculated through the *LMF scaling law* as defined by Rasmussen et al. [7]:

$$f = f_0 \frac{k_m R_{muscle1}}{k_L R_{muscle0}} \quad (4)$$

where f_0 is the unscaled nominal strength of the muscle, and k_m is the mass ratio defined as; $k_m = \frac{m_1}{m_0}$ and k_L is the length ratio defined as; $k_L = \frac{L_1}{L_0}$ between the unscaled segment (denoted 0) and the subject-specific segment (denoted 1), respectively. $R_{muscles}$ is the muscle mass proportion of the total body mass, found by; $R_{muscles} = 1 - R_{fat} - R_{other}$, where R_{other} is the proportion of the total body mass accounted for by factors such as bone, blood, and tissue, and is set to 50% in the AMS [7]. R_{fat} is the body fat percentage and is defined by Frankenfield et al. [36]:

$$R_{fat} = -0.09 + 0.0149BMI - 0.00009BMI^2 \quad (5a)$$

$$R_{fat} = -0.08 + 0.0203BMI - 0.000156BMI^2 \quad (5b)$$

where equation 5a and 5b is for male and female, respectively, and BMI is the body mass index.

Optimization based strength-scaling

The general goal of the optimization process was to estimate a set of strength factors capable of scaling all included muscle models to match each participant's 1RM measures. Practicality was highly prioritized

throughout the workflow development, why an optimization problem including all 918 muscle models as design variables was deemed unmanageable. The number of design variables were lowered to 10 (i.e. one per exercise) by; first assuming symmetry between the right and left side of the models reduced the total number of muscle models to 459. Second, a measure of how much mass the models could move during the exercise movements (equation 6), combined with a sensitivity matrix of how each muscle was active in each exercise (equation 8).

Measuring current model strength

The dynamic exercise models were fixed in a static posture equal to where the peak envelope of maximum muscle activity (a) occurred, which limited the inverse dynamics calculation to one time step. The assumption that the exercise movement can be reduced to a single posture or point in the concentric part of the movement, is based on the idea of a “sticking point” or “sticking region”, which is used extensively in the strength exercise literature [37–39]. It is defined as the point at which muscular failure is most likely to occur. Overcoming this point is associated with completing the full repetition. The phenomenon has proven to be difficult to assess on an inter-subject level due to morphological differences between subjects [38].

After creating a static scenario for each model, the relationship between applied mass (m) [kg] and a was investigated. The analysis showed that, for m above an exercise-specific threshold, the relationship can be assumed linear in the form; $y = \alpha x + \beta$, where α denote the slope calculated as; $\alpha = \frac{x_2 - x_1}{y_2 - y_1}$ using two (x, y) coordinates on the line, and β denote the y -axis intercept. This linearity stems from using the min/max muscle recruitment criterion during the inverse dynamics analysis, where the linear relationship has been shown between the external moment and muscle activity [21]. Further, for all exercises the assumed linearity crosses $a = 1$, indicating that when running two model simulations, using two applied masses high enough to be on the linear section, the applied mass (m) where $a = 1$ can be calculated as:

$$1\widehat{RM} = \frac{1}{\alpha} - \frac{a}{\alpha} + m \quad (6)$$

where $1\widehat{RM}$ is the current estimated $1RM$ for the models and will serve as part of the objective function for the optimization problem.

Formulating an optimization problem

An unconstrained minimization problem was formulated using the objective function:

$$J = \sum_{i=1}^n \left(1\widehat{RM}_i - 1RM_i \right)^2 \quad (7)$$

where n denotes the number of exercises and i denotes the i^{th} exercise. The optimization workflow was written in Python 3.7 (Python Software Foundation, Beaverton, Or, USA) using the Nlopt package [40] and the NEWUOA BOUND quadratic approximation algorithm [41].

Calculating strength factors

The general idea behind the use of a multitude of exercises targeting different muscle groups was the ability to create a $m_{exercises} \times n_{muscles}$ sensitivity matrix (\mathbf{M}) of how a change in each muscle’s nominal strength (Δf) [N] affects the a . The sensitivity measure was formulated as:

$$\mathbf{M} = \sum_{i=1}^n \frac{\Delta a_i}{\Delta f_i} \quad (8)$$

Since an overlap in muscles working in each strength exercise is unavoidable, a correlation exists between the a in each exercise. This correlation could be a limiting factor in the optimization and was sought to be resolved by invoking a PCA on the sensitivity matrix and using the orthogonal principal components (\mathbf{D}) in the further analysis. A linear equation system was formulated to solve for the strength factors (k_{mus}) to implement:

$$k_{mus} = \mathbf{D}\kappa + k_0 \quad (9)$$

where k_0 is a vector of ones and κ is the design variables used in the optimization. The strength factors were parsed to the AMS models, effectively multiplied to each muscle’s nominal strength (f_0), and a new $1\widehat{RM}$ was evaluated by the optimizer using equation 6.

Data analysis

A baseline scaling was used in comparison with the novel SS workflow. This consisted of geometrically scaling the exercise models to the participant’s anthropometrics and calculating their $1\widehat{RM}$ using the underlying LMF SS as a standard-scaled model (LMF_{SS}). To evaluate the accuracy of the subject-specific SS relative to the subject-specific $1RM$ for

each participant, a normalized root mean squared error (NRMSE) was calculated for both the LMF_{SS} and the novel optimization based SS (OPT_{SS}) models:

$$NRMSE = \sqrt{\frac{1}{n} \sum_{i=1}^n \left(\frac{\widehat{1RM}_i - 1RM_i}{1RM_i} \right)^2} 100 \quad (10)$$

Further, a pooled accuracy measure was calculated as the mean NRMSE of all included participants to evaluate the workflow in general. An analysis of how the OPT_{SS} affected the envelope of muscle activity across the dynamic exercise movements was evaluated by investigating if the sticking point used for the optimization, and the muscle activity across the full dynamic ROM, had changed after applying the OPT_{SS} .

Part 2

The second part of the study focused on validating the results obtained in part 1, using isometric strength assessment of specific joint movements. Since the field tested strength exercises require different amounts of technique and stabilization, the elbow flexion and extension, knee flexion and extension, and ankle plantar flexion, i.e. the simplest ones, were chosen for comparison.

Protocol

The experiment was conducted at the strength laboratory at Aalborg University using a Human Norm model 770 dynamometer (Computer Sports Medicine Inc., Stoughton, MA, USA). 13 participants from the verification experiment were recruited, and consisted of 10 males and 3 females, with a mean (\pm SD) age of 26.31 (\pm 1.80) years, stature of 1.83 (\pm 0.08) m, and body mass of 96.84 (\pm 22.25) kg. The participants reported to the laboratory for one session and started with an introduction to the protocol and a 10-minute general full-body dynamic mobility warm-up. The order of exercises was; ankle plantar flexion, elbow extension, elbow flexion, knee flexion, and knee extension. For all movements only the right side was tested, in line with the protocol from the part 1. The participants were tested while supine for the ankle and both elbow movements, prone for the knee flexion movement, and seated for the knee extension movement. The anatomical axis of rotation for the tested joint, was aligned with the dynamometer axis of rotation using visual inspection and manual palpation. Further, each testing angle was determined by the sticking point location found during part 1 (table 1). After alignment and safely securing the participant, a

series of five submaximum trials served as a specific warm-up and familiarization to the movement. The participants were instructed to perform the submaximum voluntary contractions for three seconds, with each trial separated by 15 seconds of rest, and an additional 45 seconds of rest before the testing trials. The participants performed three maximal voluntary contractions (MVC) for five seconds, each separated by one minute of rest. Verbal encouragement was given during all MVC trials. Two minutes rest separated each of the five movements.

Table 1: Angles [$^{\circ}$] for maximum voluntary contraction for each movement. Ankle plantar flexion is denoted as ankle flexion.

Joint	Flexion	Extension
Elbow	30	73
Knee	5	5
Ankle	-14	

Isometric strength models

For the validation experiment, the AMS *EvaluateJointStrength* class was implemented to estimate the PJT of the LMF_{SS} (\widehat{PJT}_{LMF}) and OPT_{SS} (\widehat{PJT}_{OPT}), respectively. The tested joints were positioned corresponding to the dynamometer tests, and all other degrees of freedom were carried by reaction forces.

Data analysis

The gravitational corrected dynamometer torque data was exported for further analysis. A custom Python script was written to extract the PJT and calculate a mean across the participant's three MVC trials. The PJT means were compared to the \widehat{PJT}_{LMF} and the \widehat{PJT}_{OPT} , respectively. The comparison was done through Bland-Altman plots, including bias and limits of agreement (LoA). The hypothesis was that the OPT_{SS} would show more narrow LoA and a lower mean bias between PJT , when comparing lab results with model performance.

Results

The mean NRMSE across all 28 participants for each exercise, for the LMF_{SS} and OPT_{SS} , is shown in table 2. The NRMSE can be interpreted as the average percentage deviation of the $\widehat{1RM}$ from the field obtained 1RM. The results shows that the OPT_{SS} is effective in reducing the mean NRMSE across all exercises from 48.39 (\pm 22.99) % to 28.13 (\pm 15.47) %.

Moreover, table 2 shows that the OPT_{SS} is most effectively scaling the calf raise exercise, lowering the NRMSE from 70.4 % to 11.5 %. The lateral raise exercise is on average deviating 66.4 %, making it the least accurately optimized exercise.

Table 2: Normalized root mean square error (NRMSE) [%] for each exercise and a mean and SD across all exercises, for the standard scaled (LMF_{SS}) and the optimization scaled (OPT_{SS}) models, respectively.

	NRMSE	
	LMF_{SS}	OPT_{SS}
Bench press	25.0	15.8
Biceps curl	34.2	24.7
Calf raise	70.4	11.5
Horizontal row	29.7	21.4
Lateral raise	101.0	66.4
Lateral pulldown	33.5	31.2
Leg curl	40.3	29.0
Leg extension	46.8	18.4
Side bends	58.3	25.5
Triceps extension	44.7	37.6
Mean	48.39	28.13
SD	22.99	15.47

Table 3 shows how each participant is scaled by the OPT_{SS} workflow. It is shown that the OPT_{SS} is effective in improving the NRMSE for all participants but one (p_{04}). The OPT_{SS} performs best for p_{18} improving the NRMSE from 46.78% to 5.35% and for p_{27} the OPT_{SS} results in a NRMSE improvement of 0.65%. When investigating the time to convergence (TTC) in table 3, the optimization time ranges from 33 minutes to 8 hours and 43 minutes, with an average of 2 hours and 35 minutes. Further, table 3 shows the participants' descriptives, where the majority of the participants had either 2 or 5 years of experience with strength training throughout the past five years (10 and 9 participants, respectively). At the time of the field strength test 15 participants were doing training less than 1-2 times per week, and two participants were training more than five times per week.

Figure 1 shows a graph of the dynamic full ROM for each exercise used to identify the peak a . The graph is created using the $1RM$ from one participant (p_{01}) applied to the full ROM. This was done for both the LMF_{SS} and OPT_{SS} , with their corresponding masses. The figure shows how the sticking point is affected by implementing the strength factors based on the OPT_{SS} . Imposing the OPT_{SS} has an effect on the sticking point location especially for the biceps curl, horizontal row, and side bends exercises.

Furthermore, the figure shows when the posture of the calf raise and lateral pulldown exercises is fixed, the muscle activity either increases (seen in the lateral pulldown exercise) or decreases (seen in the calf raise exercise).

Table 4 shows the PJT obtained from the dynamometer experiment, and the AMS *Evaluate-JointStrength* studies when applying the LMF_{SS} and OPT_{SS} , respectively. Further, figure 2 shows a Bland-Altman plot for each of the movements from part 2. It shows a mean bias below 10 Nm for the elbow joint, while the knee and ankle joint shows a mean bias of more than 950 and 250 Nm, respectively.

Discussion

Part 1

The scope of the present study was separated into two, where the first aim was to create and verify a workflow to perform subject-specific SS of musculoskeletal models. When analysing the overall results from the optimization routine, it is clear that the OPT_{SS} represent the participants' 1RM better than the standard LMF_{SS} . It is effectively improving the NRMSE across all participants except for p_{04} (table 3). Furthermore, when investigating the participant's descriptives in table 3, no immediate link exists between the optimization results and the influence of gender, BMI and R_{fat} , experience with strength exercises, or the amount of strength training performed per week. This could indicate that the workflow is robust and increases the accuracy across the population sample. Although effort was put into recruiting participants of both anthropometric differences and variations in strength exercise experience. Table 3 shows that only four participants had no experience with strength training and that the average experience in the past five years was 2.89 (± 1.81) years, indicating that the present population was above average experienced (> 2.5 years). The relatively high experience level could hide certain side effects, such as novice participants focusing more on maintaining exercise technique, or not having experience with maximal force production (i.e. the ability to recruit large motor units). Including more untrained participants could clarify if some of the included exercises might have been too difficult to perform, and thereby hard to accurately measure strength.

Table 3: Participants’ descriptives including; gender (GEN) [m=male, f=female], body mass index (BMI), estimated body fat percentage (R_{fat}), strength training experience during the last five years (EXP) [years], training sessions per week (TSPW) indexed as: never, rarely, 1-2, 3-4, and 5+. Furthermore, the optimization descriptives including; objective function value (J), function evaluations (nEval), time to convergence (TTC) [HH:MM], and normalized root mean square error (NRMSE) across all exercises for the standard-scaled (LMF_{SS}) and optimization based (OPT_{SS}) conditions, respectively.

Participant	Participants’ Descriptives					Optimization descriptives				
	GEN	BMI	R_{fat}	EXP	TSPW	J	nEval	TTC	NRMSE LMF_{SS}	NRMSE OPT_{SS}
p_{01}	m	25	22.86	4	Never	351.5	71	01:43	56.44	17.87
p_{02}	m	39	35.34	4	Never	2001.6	120	02:57	62.38	42.82
p_{03}	f	31	39.94	0	Never	389.9	90	02:23	73.83	36.31
p_{04}	m	25	23.08	5	1-2	4105.3	24	00:33	43.68	47.24
p_{05}	m	30	27.20	0	Never	237.8	122	02:59	40.99	21.91
p_{06}	f	22	29.25	0	Never	58.1	132	03:14	48.09	24.35
p_{07}	m	31	28.82	5	1-2	6550.5	30	00:43	51.07	47.31
p_{08}	m	20	17.37	2	Rarely	257.1	50	01:12	79.75	34.25
p_{09}	f	26	34.74	1	Rarely	849.9	49	01:11	59.85	31.39
p_{10}	m	26	23.37	2	1-2	165.3	150	03:40	51.80	10.58
p_{11}	m	22	19.23	2	1-2	1711.5	48	01:09	49.15	28.05
p_{12}	m	27	24.31	5	3-4	3706.3	80	01:56	44.99	33.62
p_{13}	f	29	37.68	2	5+	392.5	352	08:43	67.68	40.82
p_{14}	m	30	27.28	0	Never	626.2	35	00:50	60.94	42.45
p_{15}	m	35	31.97	5	3-4	29207.5	27	00:38	59.18	49.63
p_{16}	f	25	33.20	2	3-4	54.5	130	03:13	53.78	23.12
p_{17}	m	29	26.46	5	3-4	10885.9	88	02:08	47.98	38.21
p_{18}	f	22	28.56	2	3-4	3.6	220	05:23	46.78	5.35
p_{19}	m	27	25.05	5	3-4	94.8	200	04:56	39.72	8.87
p_{20}	f	26	34.34	5	1-2	145.9	173	04:23	52.99	24.02
p_{21}	m	30	27.75	2	Never	2749.1	117	02:52	47.61	22.52
p_{22}	m	24	21.15	3	Rarely	147.1	120	02:56	46.49	11.41
p_{23}	m	28	25.72	2	Rarely	469.2	61	01:28	45.13	12.43
p_{24}	m	28	26.03	2	Rarely	1073.9	61	01:36	39.32	16.57
p_{25}	m	23	20.32	4	Rarely	460.2	27	00:38	52.63	45.04
p_{26}	m	25	22.18	5	5+	901.9	113	02:46	44.07	16.87
p_{27}	m	32	29.39	5	Rarely	6994.7	90	02:11	52.92	52.27
p_{28}	m	27	25.08	2	Rarely	258.4	162	04:00	41.04	16.24
Mean	-	27.28	27.42	2.89	-	-	105.1	02:35	52.15	28.63
SD	-	4.16	5.64	1.81	-	-	72.1	01:47	10.03	13.93

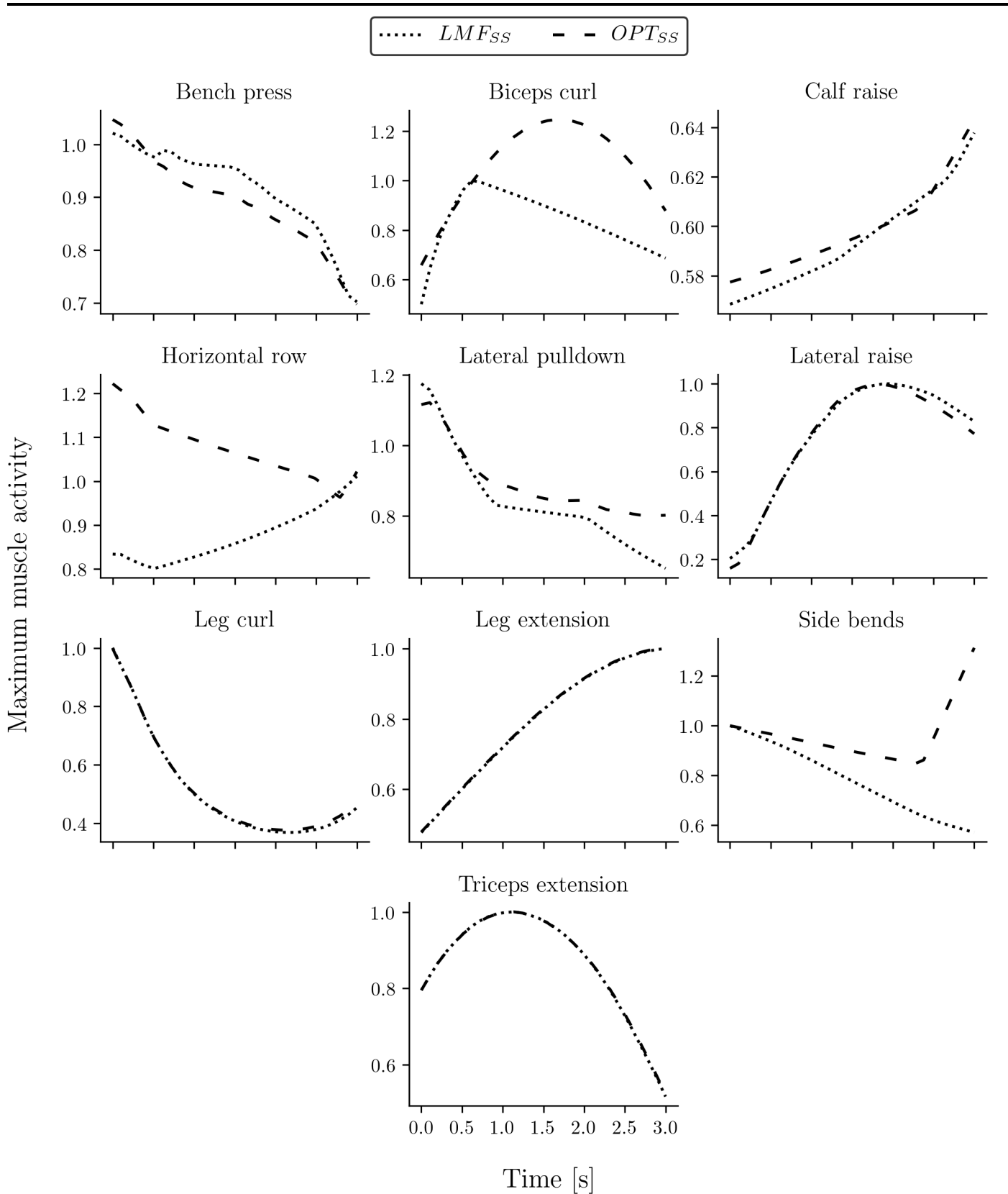
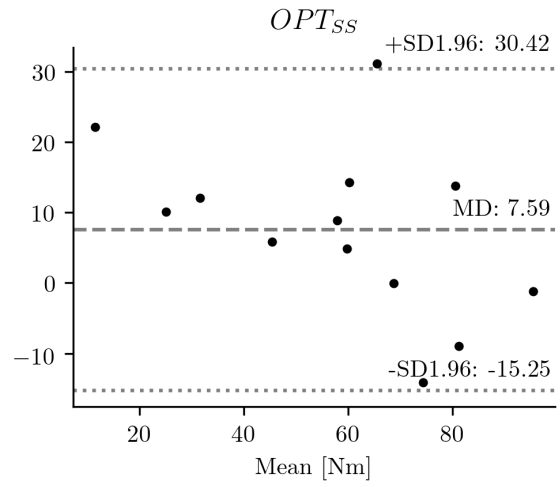
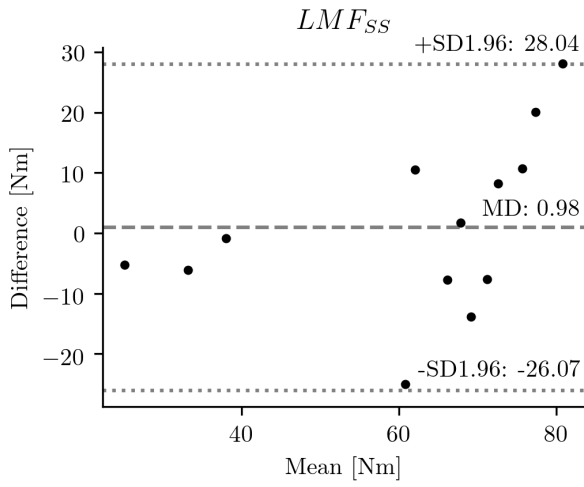


Figure 1: Maximum muscle activity during each dynamic contraction for both standard scaled (LMF_{SS}) and the optimization based (OPT_{SS}) models, respectively. Peaks indicate the location of the sticking point.

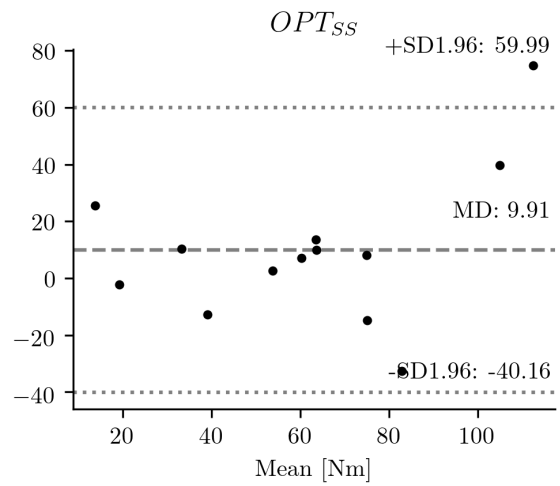
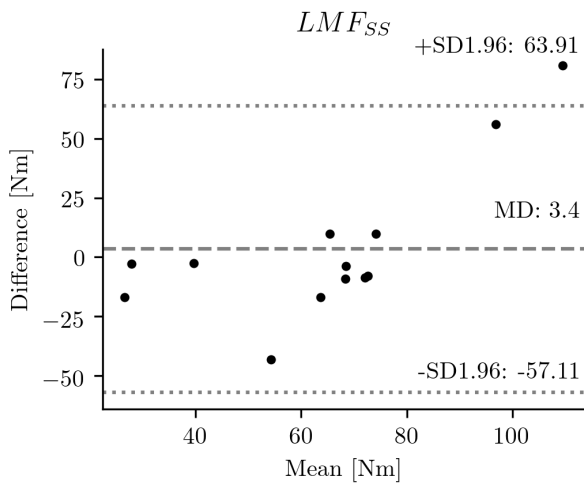
Table 4: Peak joint torques [Nm] for each participant (p) for the dynamometer (DYNO), standard scaled (LMF_{SS}) and optimization based (OPT_{SS}) conditions, respectively. Ankle plantar flexion is denoted as ankle flexion.

	Elbow flexion		Elbow extension		Knee flexion		Knee extension		Ankle flexion				
	DYNO	LMF_{SS}	LMF_{SS}	OPT_{SS}	DYNO	LMF_{SS}	OPT_{SS}	DYNO	LMF_{SS}	OPT_{SS}			
p_{01}	62.3	76.1	68.6	57.4	99.8	306.3	351.5	180.8	1244.5	1244.6	211.0	523.9	518.8
p_{02}	67.3	56.8	70.3	53.1	110.2	320.5	282.6	135.1	1053.7	1040.9	231.9	486.5	490.8
p_{03}	22.5	27.8	26.5	0.4	55.6	120.6	152.3	58.3	470.5	519.6	136.0	203.1	197.7
p_{07}	67.4	75.1	67.7	81.5	114.4	312.7	273.2	131.5	1224.4	1223.8	140.6	560.8	565.1
p_{08}	48.3	73.3	32.7	42.5	45.1	305.2	257.7	64.0	1149.4	1161.8	164.0	463.9	462.2
p_{09}	30.1	36.2	18.1	20.0	55.9	126.1	107.9	47.4	595.4	597.5	128.8	266.5	266.6
p_{15}	76.7	68.5	124.8	85.7	159.4	332.6	247.1	91.1	1214.3	1198.4	290.1	474.1	474.5
p_{17}	87.4	67.3	149.8	73.6	127.0	300.7	159.4	123.4	1181.4	1206.2	168.1	494.2	493.2
p_{18}	37.6	38.5	38.4	25.6	51.2	119.8	135.5	58.0	669.3	709.7	128.7	311.3	309.2
p_{21}	68.7	67.0	79.0	68.7	107.3	302.9	398.6	86.7	1170.5	1238.3	237.1	543.1	535.2
p_{22}	81.1	70.4	55.1	49.9	99.0	308.3	382.2	85.7	1256.3	1331.0	237.4	537.1	531.9
p_{23}	62.3	70.0	63.8	53.4	90.0	322.2	345.5	80.7	1293.8	1320.6	192.5	483.9	479.9
p_{27}	94.9	66.8	66.5	96.1	187.6	335.7	289.1	119.5	1257.9	1215.7	287.7	556.1	555.1

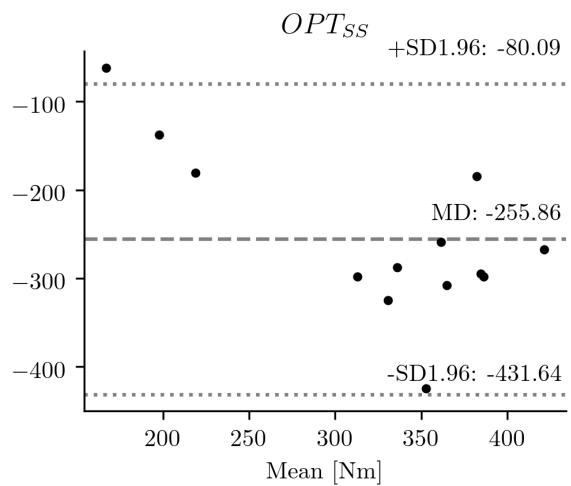
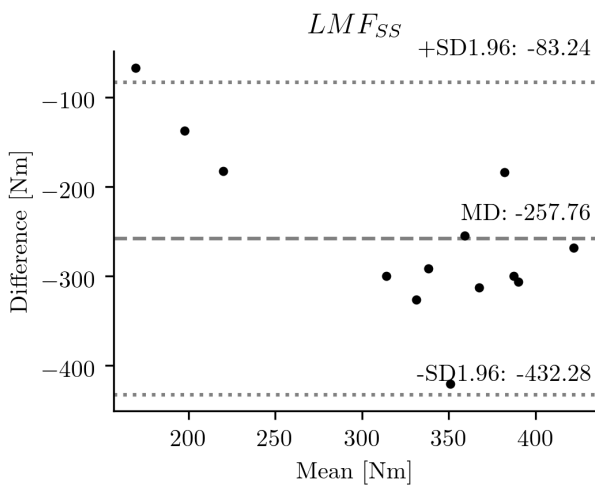
Elbow Flexion



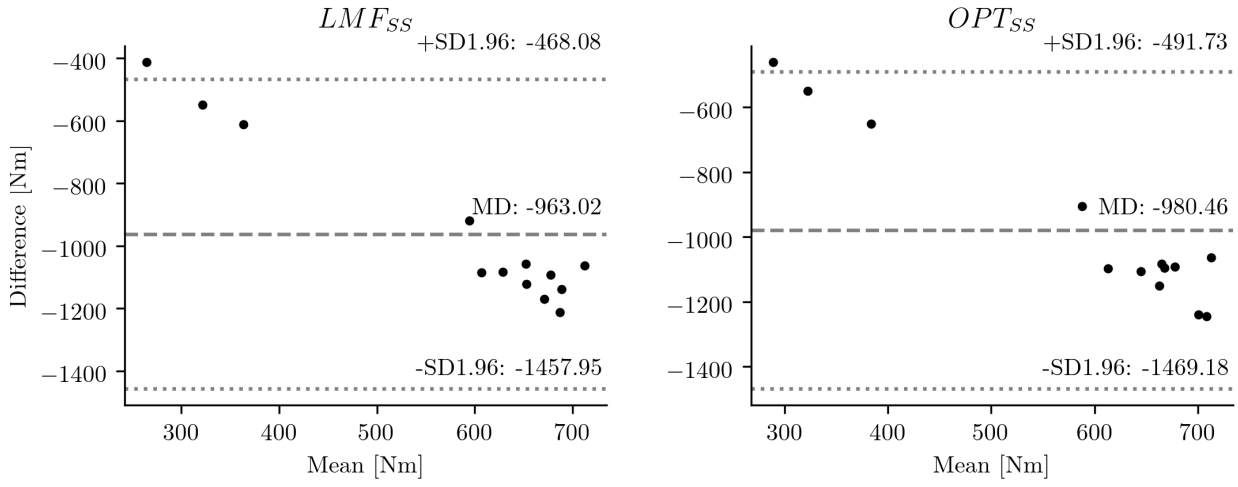
Elbow Extension



Ankle Flexion



Knee Extension



Knee Flexion

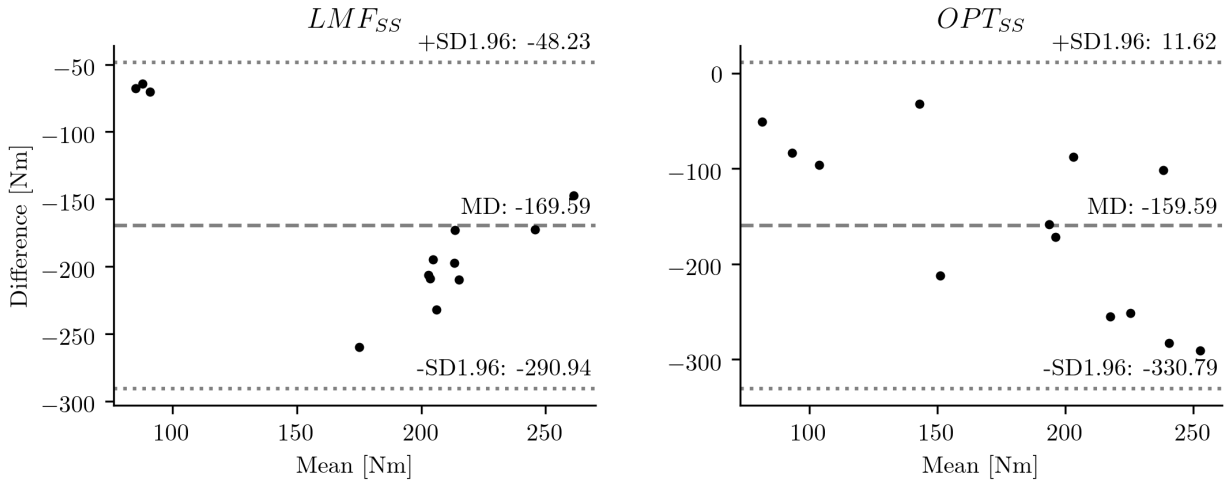


Figure 2: Bland-Altman plots for each movement tested in the validation experiment, comparing the standard scaled (LMF_{SS}) or the optimization based (OPT_{SS}) conditions' peak joint torques to the dynamometer obtained peak joint torques, left and right respectively. y -axis indicate the difference between dynamometer and either LMF_{SS} or OPT_{SS} and x -axis indicate the mean between dynamometer and either LMF_{SS} or OPT_{SS} . Dotted lines indicate limits of agreement, dashed line indicate the bias (MD = mean difference).

The OPT_{SS} routine took on average 2 hours and 35 minutes to converge, using an average of 105 iterations per participant. Comparing these numbers with the results of Heinen et al [13], whose isometric optimization routine converged after 300 iterations, the present study offers a faster and simpler method for subject-specific SS. Moreover, the maximum strength assessment used in the present study is more accessible to obtain than measuring isometric or iso-velocity strength. The use of 1RM measures to assess maximum strength is the most common method in the strength training society. Most participants which regularly engage in strength training are familiar with these measures and base their strength training progression on fractions of either measured or estimated 1RM. Further, estimating 1RM from 3-7 repetition-maximum is an applicable method for participants with little to no prior experience with strength training, since there is a lowered risk of injury compared to measuring 1RM.

Although the overall results improved for all but one participants, the accuracy of the strength optimization is only deemed satisfying for participant 18 and 19. For the workflow to be truly accurate, the NRMSE should be below 10% for any participant. When the NRMSE is below this threshold, the remaining variation is most likely lower than what can be accounted for by the precision of the regression formula, tolerances of the different weight plates and dumbbells used, or fluctuations in dietary and sleep patterns. Since no immediate variation in the optimization results could be identified from variations in participant descriptives, further improvements in accuracy would most likely derive from altering the assumptions and workflow setup.

Table 2 shows that not all exercises are equally improved by the optimization routine. A possible explanation regarding the optimization accuracy is that the algorithm does not have enough freedom to adjust the design variables to match the strength of each participant. Several steps along the workflow could be the cause of this. The characterization of exercises could influence how each muscle is affected by the optimization. Care was taken in modeling exercises without having multiple exercises testing the same major skeletal muscle groups. This is a difficult task and some overlap is unavoidable. For example, the biceps brachii muscles are involved in flexing the elbow joint and thereby contributing in the biceps curl exercise and both pulling exercises (i.e. lateral pull-down and horizontal row). The pulling exercises were

included to target the large latissimus dorsi muscles during the horizontal row, and the smaller upper back muscles (e.g. trapezius and rhomboid) alongside the rotator cuff muscles during lateral pulldown. In order to overcome these overlaps in muscle activities between exercises, a PCA was performed on the sensitivity matrix \mathbf{A} . This created orthogonal principal components and de-correlated each of the exercises' sensitivity measures.

Since the basis for obtaining the correct strength factors is derived from the sensitivity matrix \mathbf{A} , obtaining a better sensitivity measure could improve the results. One method could be to use cutoff values for the active muscles in each exercise. This would ensure that only muscles active above a certain threshold would contribute to the sensitivity matrix. This method could alleviate the issue with the biceps brachii muscles, by removing its contribution from the exercises where it is not assumed to be the main contributor. This would effectively have the optimization algorithm scale the biceps brachii strength solely from the biceps curl exercise, and thereby scaling the otherwise intended muscles from the horizontal row and lateral pulldown exercises separately. The same scenario could be true for the lateral raise exercise, which isolates and almost solely activates the deltoid and rotator cuff muscles. However, these muscles are also heavily involved during many of the other included exercises (e.g. bench press). Raising a dumbbell in a straight arm means that even relatively low loads create a large moment around the glenohumeral joint, resulting in a relatively low 1RM in the range of 5.8 – 19.7 kg. The LMF_{SS} model strength ($\widehat{1RM}$) for the lateral raise exercise is ranging from 8.4 – 34 kg, meaning that the optimizer would have to down-scale the strength of the targeted deltoid muscles to reduce this difference. Since the deltoideus muscles are involved in exercises such as the bench press, and thereby effectively contributing to the sensitivity matrix in that exercise, the optimization algorithm might try to adjust the strength of the deltoideus muscles resulting in too strong muscles when simulating the lateral raise exercise. Using another sensitivity measure could potentially improve how the optimization algorithm determines the SS. Currently, the \mathbf{A} matrix shows how a small change in muscle strength affects the muscle activity envelope for each exercise. The matrix is constructed utilizing the min/max muscle recruitment criterion. This criterion effectively postpone fatigue by allowing all contributing muscles, to contribute to their full extent. Although there is a

clear upside to using this criterion when investigating maximum strength, using it for the sensitivity matrix construction might not be the most favorable choice, due to how it recruits available muscles. Constructing the sensitivity matrix using another muscle recruitment criterion could result in a more physiological accurate representation of how the muscles are active in each exercise.

Another limitation of the optimization workflow could be associated with SS during a static posture (i.e. the sticking point position). As seen in figure 1, the location of the sticking point changes after applying the optimized strength factors. It was revealed that changing from a dynamic repetition, to a static posture, had a negative impact on 5 of the 10 exercises. No difference was found between the LMF_{SS} and OPT_{SS} conditions for the bench press, lateral raise, leg curl, leg extension, and triceps extension exercises. This indicates the optimization routine is accurately representing the strength of the active muscles in these exercises, without altering the strength relationship between muscles. The peak a for the dynamic ROM and static position equals 1, which indicate that moving from a dynamic scenario to a static posture does not affect the location of the peak a . Contradictory, the calf raise and lateral pulldown exercises are seemingly poor choices, even though the mass applied corresponded to $a = 1$ for the static position. However, the a for both SS conditions are ~ 0.64 and ~ 1.2 when performing the dynamic ROM, for calf raise and lateral pulldown respectively. For the side bends and biceps curl exercises the sticking point location is largely affected by using the OPT_{SS} condition. However, for the OPT_{SS} condition some muscles are scaled through other exercises, which could affect muscles used in other parts of the exercise ROM, resulting in a new sticking point posture. The same can be seen for the horizontal row, where the sticking point position occurs in the beginning of the movement, rather than the end. This could indicate that the muscles used in this movement is not scaled solely from this exercise. To summarize, for half of the exercises, the calculated maximal applied mass the model can sustain, is affected by switching from a dynamic scenario to a static one. Using multiple postures during the optimization might limit the variation between muscle activity when applying new strength factors.

Part 2

The second aim of the present study was to validate the strength-scaled models using dynamometer

obtained isometric joint torque measurements. The results showed that the \widehat{PJT}_{OPT} performed poorly across all isometric exercises, when compared to the golden standard (dynamometer PJT). Knee extension overestimated the \widehat{PJT} values almost by a factor of 10 for all participants, for both the \widehat{PJT}_{LMF} and \widehat{PJT}_{OPT} . Ankle plantar flexion and knee flexion overestimated the PJT values by a factor of 2-4 (table 4). These overestimations are thought to be caused by using the simple muscle models in the AMS exercise models. These muscle models do not have a force-length or force-velocity relationship and rely solely on the nominal strength parameter. This effectively means that the moment is only governed by the moment arm of each muscle. Switching to the more complex 3E muscle model, with a force-length and force-velocity relationship, showed a decrease in \widehat{PJT}_{LMF} by a factor of 4-6 for the knee extension (data not shown). Issues in the simple muscle models wrapping around the knee and ankle joint surfaces could further cause the muscle moment arms to be prone to errors. Dzialo et al. [42] showed that by modeling the knee joint with a moving rotation axis, secondary joint kinematics could be improved, indicating that the simple hinge knee joint model might also be a limiting factor when comparing PJT. For elbow flexion and extension, the comparison between the \widehat{PJT}_{LMF} , \widehat{PJT}_{OPT} and the dynamometer seems more reasonable. However, both the \widehat{PJT}_{LMF} and \widehat{PJT}_{OPT} still performed poorly when compared with the PJT values from the dynamometer. The LoA tend to get more narrow when using the \widehat{PJT}_{OPT} values, however it comes at the cost of an increased bias from 0.98 to 7.59 Nm and 3.4 to 9.91 Nm for the elbow flexion and extension, respectively. The poor performance of the OPT_{SS} during elbow extension could be influenced by how inadequately the optimization routine scaled the participants' strength in the triceps extension exercise. The NRMSE values for the triceps extension shows a 37 % mean variation between the OPT_{SS} model $1\widehat{RM}$ and field obtained 1RM. Considering p_{03} 's results from table 4, it is clear that the optimization routine had an issue when scaling the muscles crossing the elbow joint. The $1\widehat{RM}$ for p_{03} in the triceps extension exercise is only 2.6 kg, while the actual field obtained 1RM was 8.3 kg (data not shown). This further indicates that the exercises are too similar, and that an overlap in active muscles exist between exercises.

Practicality

As part of the present workflow, the ability to differentiate the strength between the left and right side of the AMS models was implemented. Furthermore, other 1RM regression formulas or even exercise-specific formulas is easily implementable if desired. The present workflow is scalable and more strength exercises can be implemented with ease, which makes the workflow practical in the sense that coaches and athletes could implement specific exercises in a custom SS optimization.

Conclusion

The present study shows promising initial results regarding the use of easily obtainable maximum strength measures to scale whole body musculoskeletal models. The improvements shown in the present study evoke confidence that further research involv-

ing the correct measure of muscle sensitivity, strength exercises to characterize the skeletal muscle actions, and the implementation of PCA combined with an optimization routine can converge to a reliable and accurate method of subject-specific SS. Further, The present study shows that utilizing simple musculoskeletal muscle models cannot readily be used to estimate and compare peak joint torque for near end ROM angles. The present field strength data and dynamometer torque data collected will be available on Zenodo for other researchers.

Acknowledgement

The authors would like to thank Mark de Zee Ph.D. and John Rasmussen Ph.D. for their supervision throughout the process. Further, a special thanks to all the employees at AnyBody Technology A/S for the countless hours spent helping with exercise model building and troubleshooting.

References

- [1] M. A. Marra, V. Vanheule, R. Fluit, B. H. F. J. M. Koopman, J. Rasmussen, N. Verdonschot, and M. S. Andersen, "A subject-specific musculoskeletal modeling framework to predict in vivo mechanics of total knee arthroplasty," en, *J. Biomech. Eng.*, vol. 137, no. 2, p. 020904, Feb. 2015, ISSN: 0148-0731, 1528-8951. DOI: 10.1115/1.4029258.
- [2] J. W. Fernandez and M. G. Pandy, "Integrating modelling and experiments to assess dynamic musculoskeletal function in humans," en, *Exp. Physiol.*, vol. 91, no. 2, pp. 371–382, Mar. 2006, ISSN: 0958-0670. DOI: 10.1113/expphysiol.2005.031047.
- [3] V. Carbone, R. Fluit, P. Pellikaan, M. M. van der Krogt, D. Janssen, M. Damsgaard, L. Vigneron, T. Feilkas, H. F. J. M. Koopman, and N. Verdonschot, "TLEM 2.0 - a comprehensive musculoskeletal geometry dataset for subject-specific modeling of lower extremity," en, *J. Biomech.*, vol. 48, no. 5, pp. 734–741, Mar. 2015, ISSN: 0021-9290, 1873-2380. DOI: 10.1016/j.jbiomech.2014.12.034.
- [4] A. Erdemir, S. McLean, W. Herzog, and A. J. Van den Bogert, "Model-based estimation of muscle forces exerted during movements," *Clin. Biomech.*, vol. 22, no. 2, pp. 131–154, 2007, ISSN: 0268-0033. DOI: 10.1016/j.clinbiomech.2006.09.005.
- [5] S. L. Delp, F. C. Anderson, A. S. Arnold, P. Loan, A. Habib, C. T. John, E. Guendelman, and D. G. Thelen, "OpenSim: Open-source software to create and analyze dynamic simulations of movement," en, *IEEE Trans. Biomed. Eng.*, vol. 54, no. 11, pp. 1940–1950, Nov. 2007, ISSN: 0018-9294. DOI: 10.1109/TBME.2007.901024.
- [6] M. Damsgaard, J. Rasmussen, S. T. Christensen, E. Surma, and M. de Zee, "Analysis of musculoskeletal systems in the AnyBody modeling system," *Simulation Modelling Practice and Theory*, vol. 14, no. 8, pp. 1100–1111, Nov. 2006, ISSN: 1569-190X. DOI: 10.1016/j.simpat.2006.09.001.
- [7] J. Rasmussen, M. de Zee, M. Damsgaard, S. T. Christensen, C. Marek, and K. Siebertz, "A general method for scaling Musculo-Skeletal models," in *2005 International Symposium on Computer Simulation in Biomechanics, Cleveland, Ohio, USA, 2005*, 2–2 pp.
- [8] E. F. Jensen, J. Raunsbæk, J. N. Lund, T. Rahman, J. Rasmussen, and M. N. Castro, "Development and simulation of a passive upper extremity orthosis for amyoplasia," *Journal of Rehabilitation and Assistive Technologies Engineering*, vol. 5, p. 2055668318761525, Jan. 2018, ISSN: 2055-6683. DOI: 10.1177/2055668318761525.
- [9] D. S. Chander and M. P. Cavatorta, "Multi-directional one-handed strength assessments using AnyBody modeling systems," *Appl. Ergon.*, vol. 67, pp. 225–236, 2018, ISSN: 0003-6870, 1872-9126. DOI: 10.1016/j.apergo.2017.09.015.
- [10] J. Skubich and S. Piszczatowski, "Model of loadings acting on the femoral bone during gait," en, *J. Biomech.*, vol. 87, pp. 54–63, Apr. 2019, ISSN: 0021-9290, 1873-2380. DOI: 10.1016/j.jbiomech.2019.02.018.
- [11] S. D. Souza, J. Rasmussen, and A. Schwirtz, "Multiple linear regression to develop strength scaled equations for knee and elbow joints based on age, gender and segment mass," *Int. J. Human Factors Modelling and Simulation*, vol. 3, no. 1, pp. 32–47, 2012, ISSN: 1742-5549. DOI: 10.1504/IJHFMS.2012.050071.
- [12] P. Oomen, J. Annegarn, J. Rasmussen, J. Rausch, K. Siebertz, L. Verdijk, M. Drost, and K. Meijer, "Development and validation of a rule-based strength scaling method for musculoskeletal modelling," *International Journal of Human Factors Modelling and Simulation*, vol. 5, no. 1, pp. 19–32, 2015, ISSN: 1742-5549. DOI: 10.1504/IJHFMS.2015.068121.
- [13] F. Heinen, S. N. Sørensen, M. King, M. Lewis, M. E. Lund, J. Rasmussen, and M. de Zee, "Muscle-Tendon unit parameter estimation of a Hill-Type musculoskeletal model based on experimentally obtained Subject-Specific torque profiles," *J. Biomech. Eng.*, vol. 141, no. 6, p. 061005, Jun. 2019, ISSN: 0148-0731. DOI: 10.1115/1.4043356.
- [14] M. D. Klein Horsman, "The twente lower extremity model. consistent dynamic simulation of the human locomotor apparatus," Dec. 2007.

- [15] A. V. Hill, "The heat of shortening and the dynamic constants of muscle," en, *Proc. R. Soc. Lond. B Biol. Sci.*, vol. 126, no. 843, pp. 136–195, Oct. 1938, ISSN: 0080-4649, 2053-9193. DOI: 10.1098/rspb.1938.0050.
- [16] F. Heinen, M. E. Lund, J. Rasmussen, and M. de Zee, "Muscle-tendon unit scaling methods of hill-type musculoskeletal models: An overview," en, *Proc. Inst. Mech. Eng. H*, vol. 230, no. 10, pp. 976–984, Oct. 2016, ISSN: 0954-4119, 2041-3033. DOI: 10.1177/0954411916659894.
- [17] M. E. Lund, M. S. Andersen, M. de Zee, and J. Rasmussen, "Scaling of musculoskeletal models from static and dynamic trials," *International Biomechanics*, vol. 2, no. 1, pp. 1–11, 2015, ISSN: 2333-5432. DOI: 10.1080/23335432.2014.993706.
- [18] S. Skals, M. K. Jung, M. Damsgaard, and M. S. Andersen, "Prediction of ground reaction forces and moments during sports-related movements," *Multibody Syst. Dyn.*, vol. 39, no. 3, pp. 175–195, Mar. 2017, ISSN: 1384-5640, 1573-272X. DOI: 10.1007/s11044-016-9537-4.
- [19] R. Arshad, L. Angelini, T. Zander, F. Di Puccio, M. El-Rich, and H. Schmidt, "Spinal loads and trunk muscles forces during level walking - a combined in vivo and in silico study on six subjects," en, *J. Biomech.*, vol. 70, pp. 113–123, Mar. 2018, ISSN: 0021-9290, 1873-2380. DOI: 10.1016/j.jbiomech.2017.08.020.
- [20] T. Hölscher, T. Weber, I. Lazarev, C. Englert, and S. Dendorfer, "Influence of rotator cuff tears on glenohumeral stability during abduction tasks," en, *J. Orthop. Res.*, vol. 34, no. 9, pp. 1628–1635, Sep. 2016, ISSN: 0736-0266, 1554-527X. DOI: 10.1002/jor.23161.
- [21] J. Rasmussen, M. Damsgaard, and M. Voigt, "Muscle recruitment by the min/max criterion - a comparative numerical study," *J. Biomech.*, vol. 34, no. 3, pp. 409–415, 2001, ISSN: 0021-9290. DOI: 10.1016/S0021-9290(00)00191-3.
- [22] M. Inez, R. Pereira, P. Sergio, and C. Gomes, "Muscular strength and endurance tests: Reliability and prediction of one repetition maximum - review and new evidences," *Rev. Bras. Med.*, vol. 9, no. 5, pp. 336–346, 2003, ISSN: 0034-7264, 1517-8692. DOI: 10.1590/S1517-86922003000500007.
- [23] D. A. LeSuer, J. H. McCormick, J. L. Mayhew, R. L. Wasserstein, and M. D. Arnold, "The accuracy of prediction equations for estimating 1-RM performance in the bench press, squat, and deadlift," *J. Strength Cond. Res.*, vol. 11, no. 4, p. 211, Nov. 1997, ISSN: 1064-8011.
- [24] J. D. Taylor and W. D. Bandy, "Intrarater reliability of 1repetition maximum estimation in determining shoulder internal rotation muscle strength performance," *The Journal of Strength and Conditioning research*, vol. 19, no. 1, pp. 163–168, 2005.
- [25] M. Amarante, E. S. Cyrino, and F. Y. Nakamura, "Validation of the brzycki equation for the estimation of 1-RM in the bench press," *Rev. Brasil. Med. Esporte*, vol. 13, no. 1, pp. 40–42, 2007, ISSN: 1517-8692. DOI: 10.1590/S1517-86922007000100011.
- [26] A. Jiménez and J. A. De Paz, "Application of the 1rm estimation formulas from the rm in bench press in a group of physically active middle-aged women," *Journal of Human Sport & Exercise*, vol. 3, no. 1, pp. 10–22, 2008, ISSN: 1699-1605. DOI: 10.4100/jhse.2008.31.02.
- [27] M. E. Lund, M. De Zee, M. S. Andersen, and J. Rasmussen, "On validation of multibody musculoskeletal models," *Proc. Inst. Mech. Eng. H*, vol. 226, no. 2, pp. 82–94, 2012, ISSN: 0954-4119. DOI: 10.1177/0954411911431516.
- [28] K. M. Knutzen, L. R. Brilla, and D. Caine, "Validity of 1RM prediction equations for older adults," *J. Strength Cond. Res.*, vol. 13, no. 3, pp. 242–246, 1999, ISSN: 1064-8011. DOI: 10.1519/1533-4287(1999)013<0242:VOPEFO>2.0.CO;2.
- [29] M. E. Lund, S. Tørholm, and M. Jung, *The AnyBody managed model repository (AMMR)*, Jun. 2018. DOI: 10.5281/zenodo.1287730.
- [30] M. de Zee, D. Falla, D. Farina, and J. Rasmussen, "A detailed rigid-body cervical spine model based on inverse dynamics," *J. Biomech.*, vol. 40, S284, Jan. 2007, ISSN: 0021-9290. DOI: 10.1016/S0021-9290(07)70280-4.
- [31] M. de Zee, L. Hansen, C. Wong, J. Rasmussen, and E. B. Simonsen, "A generic detailed rigid-body lumbar spine model," en, *J. Biomech.*, vol. 40, no. 6, pp. 1219–1227, 2007, ISSN: 0021-9290. DOI: 10.1016/j.jbiomech.2006.05.030.
- [32] H. E. J. Veeger, B. Yu, K. N. An, and R. H. Rozendal, "Parameters for modeling the upper extremity," *J. Biomech.*, vol. 30, no. 6, pp. 647–652, 1997, ISSN: 0021-9290. DOI: 10.1016/S0021-9290(97)00011-0.
- [33] M. S. Andersen, M. Damsgaard, and J. Rasmussen, "Kinematic analysis of over-determinate biomechanical systems," *Comput. Methods Biomech. Biomed. Engin.*, vol. 12, no. 4, pp. 371–384, 2009, ISSN: 1025-5842. DOI: 10.1080/10255840802459412.
- [34] C. C. Gordon, "1988 anthropometric survey of US army personnel: Methods and summary statistics," *Technical Report Natick/TR-89/044*, 1989.
- [35] M. S. Andersen, M. Damsgaard, B. MacWilliams, and J. Rasmussen, "A computationally efficient optimisation-based method for parameter identification of kinematically determinate and over-determinate biomechanical systems," en, *Comput. Methods Biomech. Biomed. Engin.*, vol. 13, no. 2, pp. 171–183, 2010, ISSN: 1025-5842, 1476-8259. DOI: 10.1080/10255840903067080.
- [36] D. C. Frankenfield, W. A. Rowe, R. N. Cooney, J. S. Smith, and D. Becker, "Limits of body mass index to detect obesity and predict body composition," *Nutrition*, vol. 17, no. 1, pp. 26–30, 2001, ISSN: 0899-9007. DOI: 10.1016/S0899-9007(00)00471-8.
- [37] O. Arandjelović, "Optimal effort investment for overcoming the weakest point: New insights from a computational model of neuromuscular adaptation," en, *Eur. J. Appl. Physiol.*, vol. 111, no. 8, pp. 1715–1723, Aug. 2011, ISSN: 1439-6319, 1439-6327. DOI: 10.1007/s00421-010-1814-y.
- [38] J. Kompf and O. Arandjelović, "Understanding and overcoming the sticking point in resistance exercise," *Sports Med.*, vol. 46, no. 6, pp. 751–762, 2016, ISSN: 0112-1642, 1179-2035. DOI: 10.1007/s40279-015-0460-2.
- [39] R. Van Den Tillaar, V. Andersen, and A. H. Saeterbakken, "The existence of a sticking region in free weight squats," *J. Hum. Kinet.*, vol. 42, no. 1, pp. 63–71, 2014, ISSN: 1640-5544, 1899-7562. DOI: 10.2478/hukin-2014-0061.
- [40] S. G. Johnson, *The NLOpt nonlinear-optimization package*, 2014.
- [41] M. J. D. Powell, "The NEWUOA software for unconstrained optimization without derivatives," in *Large-Scale Nonlinear Optimization*, G. Di Pillo and M. Roma, Eds., Boston, MA: Springer US, 2006, pp. 255–297, ISBN: 9780387300658. DOI: 10.1007/0-387-30065-1_16.
- [42] C. M. Dzialo, P. H. Pedersen, C. W. Simonsen, K. K. Jensen, M. de Zee, and M. S. Andersen, "Development and validation of a subject-specific moving-axis tibiofemoral joint model using MRI and EOS imaging during a quasi-static lunge," en, *J. Biomech.*, vol. 72, pp. 71–80, Apr. 2018, ISSN: 0021-9290, 1873-2380. DOI: 10.1016/j.jbiomech.2018.02.032.

Worksheets

A detailed description of certain methodological topics, including problems and thoughts, will be presented in the following worksheets.

Contents

1. Exercise models	2
1.1. General information	2
1.2. Support conditions	2
1.3. The inverse dynamics study	2
1.4. Excluded models	3
1.5. Specific model information	4
1.6. Models for part 2	19
2. Subject-specific geometric scaling	20
2.1. Calculating subject-specific scaling factors	22
3. Defining the sticking point	22
4. Calculating model strength	24
5. Strength optimization	26
5.1. Introduction	26
5.2. Dependencies	26
5.3. Workflow	26
5.4. Optimization algorithm benchmark	26
5.5. Omitting the optimization	27
6. Protocol specific details	29
6.1. Fitness equipment	30
6.2. Learning effect during strength training	31
References	33

1. Exercise models

This worksheet describes the details regarding the structure and build of the included AnyBody Modeling System (AMS) strength exercise models. The first sections describes the general information regarding the creation of the exercise models and how certain aspects of the field test were translated to the AMS models. The following sections elaborates details about the specific models. A figure of both the exercise model fixed in the sticking point position from the field test and AMS is shown under each exercise subsection, figure 1-15. The general idea is to create an open source strength exercise library that can be used to further develop and test the workflow.

1.1. General information

The models were built to resemble strength exercises that can easily be performed in most fitness centers. The models only represented the concentric part of the movement, based on where the sticking point occurs [1] (see 3. *Defining the sticking point*). For generalization purposes the exercise library was modeled using simple measures, such as linear distances between segments and the global origin, or a specific range of motion (ROM) expressed through joint angles, to drive the motion of each model. This eliminates the need for subject-specific technique measurements, such as motion capture data of how a participant performs each exercise. From a commercialization point of view, it was interesting to investigate if these general models could be used across a heterogeneous population sample to scale subject-specific models. This would decrease the complexity of the workflow and the amount of subject-specific data to collect. Some of the strength exercise models implemented dumbbells, barbells and handles. It was assumed that they would not rotate, therefore, any segment held by the hand had reaction forces applied in all three rotational directions. All models were based on the human model template in the AnyBody Managed Model Repository (AMMR) ver. 2.2.0 [2]. Each model included the TLEM 2.0 leg model [3], detailed neck model [4], lumbar spine model [5], and the shoulder-arm model [6].

1.2. Support conditions

All exercise models utilized a type of support, e.g. feet placed on the ground, hand in contact with a wall, or the participant leaning against a wall. These conditions were modeled as reaction forces. The in-built *ground reaction force prediction* (GRFP) class was used in all exercises where the feet were in contact with the ground or foot rests. The class constructs 25 nodes under each foot segment and models a normal and friction force using muscle-like actuators, only capable of pushing [7]. The GRFP class makes it possible to control how much friction force the model is able to recruit, as a fraction of the normal force, while also solving the balance of the model. The GRFP actuator muscle will only make use of the ground reactions if that minimizes the overall maximum muscle activity (a). The trigger volume, which decides if the feet are close enough to enable contact, was adjusted in size, to ensure that the models' feet would always be inside. The GRFP base class *ContactSurfaceLinPush* was implemented, to simulate the participant leaning against a wall in the side bends and lateral raise exercises. This class models a normal force perpendicular to the thorax segment and a friction force parallel to the thorax segment, simulating the contact between the thorax and the wall.

1.3. The inverse dynamics study

The study section of the AMS models is where numerous key parameters is defined. Since the exercise models utilized the default drivers for all degrees of freedom, the addition of extra drivers to model the exercise ROM resulted in kinematically overdeterminate models. The AMS provides a solver (*KinSolOverDeterminate*) to overcome these scenarios based on the work of Andersen et al. [8]. All dynamic exercise movements were modeled using 30 timesteps, corresponding to a three second time period. This was chosen based on field observations of maximum contractions during the pilot test, and the notion that maximum contractions involve the contraction velocity approaching zero, thereby increasing the time of the repetition.

1.3.1. Muscle recruitment criterions

For the inverse dynamics analysis, several muscle recruitment criterions exist in the AMS. These are designed to minimize a cost function, taking into account that muscle force is produced by metabolic energy and that muscles can only pull, formulated as:

$$\begin{aligned}
& \text{minimize} && G(f^{(m)}) \\
& \text{subject to:} && \mathbf{C}f = r \\
& && f_i^{(m)} \geq 0, i = 1 \dots n^{(m)}
\end{aligned} \tag{1}$$

where G is the cost function, $f^{(m)}$ represent the muscle forces, $\mathbf{C}f = r$ is the equilibrium equations defined as a constraint, where \mathbf{C} is a matrix of coefficients, f is the muscle force and r is the external and inertia forces. The last constraint states that the muscle forces are restricted in sign, ensuring that they only pull. The task is now to determine which G is most representative of the physiological system in question. The simplest is the linear recruitment; $G = \frac{f_1}{N_1} + \frac{f_2}{N_2} \dots \frac{f_n}{N_n}$, where f_n is the muscle force of the n^{th} muscle and N_n is a normalization factor, typically the maximum force that the muscle can exert. This criterion will result in only the minimum number of muscles being recruited, based on their moment arms and strength. This criterion fails to represent how co-contraction and muscle synergy works. Another criterion is the quadratic criterion; $G = \sum_i (\frac{f_i}{N_i})^2$. This criterion is used extensively as it have been shown to represent muscle forces well during experiments [9]. A more general description of the criterion is the polynomial form; $G = \sum_i (\frac{f_i}{N_i})^p$, where AMS offers a value of the power (p) between 1 – 5, since $p > 5$ starts to resemble the min/max criterion. Changing p affects how much co-contraction the model is able to utilize, since it penalizes large terms in the recruitment. The last recruitment criterion is the min/max muscle recruitment criterion; $G = \max(\frac{f_i}{N_i})$. This is effectively the same as letting p approach infinity for polynomial criterions, as shown by Rasmussen et al. [10]. This criterion effectively postpones fatigue by letting all contributing muscles, work to the extent feasible. A side effect of both the higher order polynomial and min/max muscle recruitment criterions is that some muscles will be recruited faster than they are physiological able to in the human body. The min/max criterion is well suited for scenarios involving maximum strength, why the present study chose this criterion.

1.4. Excluded models

The initial characterization of strength exercises needed to encapsulate the gross skeletal muscles of the human body indicated that 15 models where to be included in the present study. However, five exercises were excluded from the optimization routine; the hip abduction, hip adduction, crunches, glute bridge, and hyperextension exercises. Common for these models are that they involve multiple support conditions and thereby multiple points of reaction forces working. Adding these, using the tools listed in section 1.2, resulted in the models becoming unrealistically strong, recruiting other muscles than the intended, or fail to meet the linearity criterion described in worksheet 4. *Calculating model strength*. This was especially clear in the hip abduction and adduction exercises, where reaction forces between the hand and the wall caused the model to recruit upper body muscles much more than the intended hip muscles. A solution of not applying reaction forces at the hand and instead applying a rotational fix of the thorax segment and reaction forces to the pelvis x and z directions in global coordinates, were implemented. However, this did not solve the problem with the models being too strong and inevitably lead to an exclusion.

The crunches and glute bridge exercises were modeled with 10 contact nodes added to the gluteus maximus muscle, and the T11, T9, and the scapula segments. The *ContactSurfaceLinPush* class was implemented between the nodes and the global coordinate system (GCS). These contact models should allow a smooth movement of both models which loses contact with the ground node by node. However, the a showed large peak values and rapid increases during the dynamic movements. This could indicate that 10 nodes were insufficient to create a smooth movement and further development is needed in order to include the models in the optimization routine.

After further investigation of the hyperextension model using the $\widehat{1RM}$, a clear error occurred. For some participants the model was not able to move the body mass of the participant without reaching a $a > 1$ and showed a non-linear relationship between applied mass and muscle activity. This could indicate the modeled reaction forces was not implemented correctly, and lead to the exclusion of the exercise.

1.5. Specific model information

1.5.1. Bench press

The model simulates a person supine on a bench, with the feet fixed on the ground using the GRFP class and with 90 degree knee flexion. A vertical reaction force is placed on both the skull and thorax segments, which represents the bench. The start position is modeled with the carpal segments coupled to the barbell through spherical joints, with 80 cm between them, holding the barbell ~ 5 cm above the anterior side of the sternum, inline with the T5 vertebrae. The barbell start position is determined as:

$$bar_{pos0} = wrist_y + 0.1 \quad (2)$$

where $wrist_y$ is the y coordinate of the wrist joint in global coordinates, and the constant 0.1 represent approximately half the length of the hand segment in meters added to the position of the wrist joint. This ensures that the linear path of the barbell scales accordingly to the participants' anthropometrics. The barbell moves away from the torso towards the end point where the arms are almost stretched out above the torso, with 10 degree elbow flexion. A linear measure defined as the distance between the barbell and the sternum is used to simulate the desired movement.

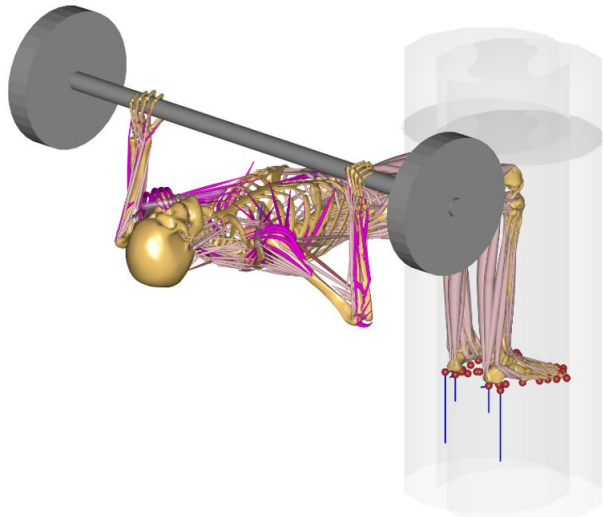


Figure 1: The sticking point position of the bench press exercise as seen in the fitness center and in the AnyBody Modeling System.

1.5.2. Biceps curl

The model simulates a person standing with their hands down the side of the body. The feet are locked in position by the GRFP class. The starting position is with the right arm stretched and the hand grabbing a machine handle, simulated by a spherical joint. The mass of the handle was set to 0.10 kg, to represent the actual mass of the handle in the fitness center. From this position the elbow is flexing towards 125 degrees, while keeping the elbow close to the body, simulating the full ROM. The force representing the cable pull force is added to the handle segment, working vertically downwards in the GCS.

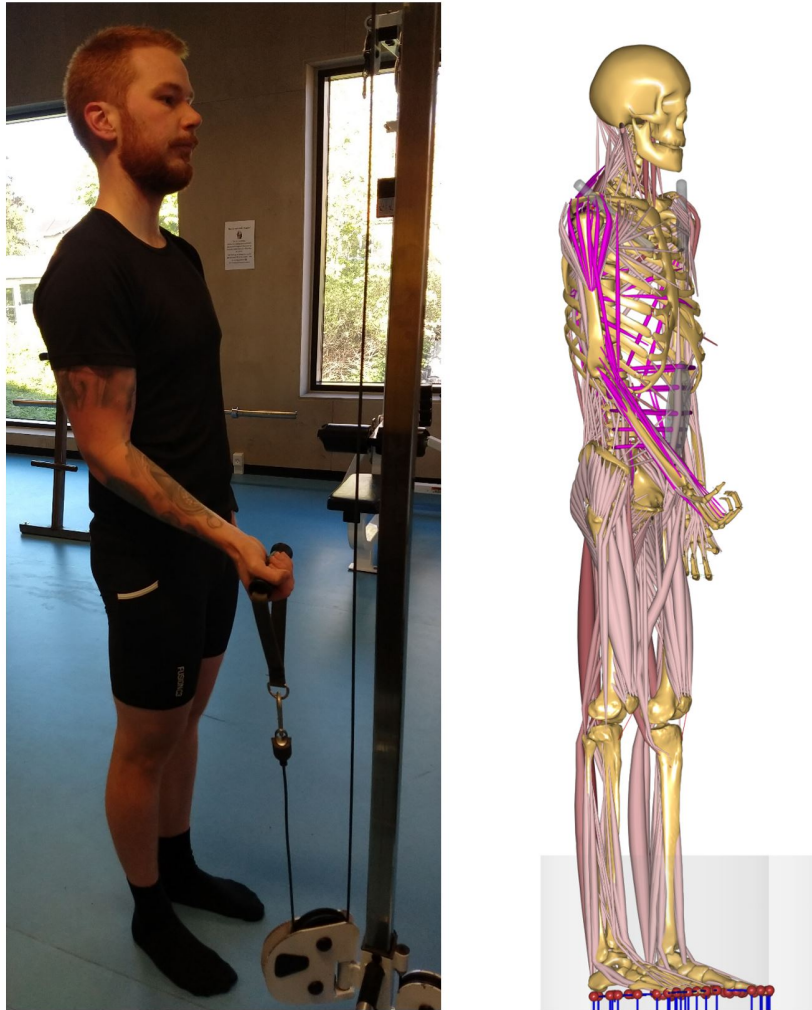


Figure 2: The sticking point position of the biceps curl exercise as seen in the fitness center and in the AnyBody Modeling System.

1.5.3. Calf raise

The model simulates a person standing upright in a smith rack with the right forefoot on a ledge. The contact between the forefoot and the ledge is simulated by altering the GRFP class slightly to only incorporate the 13 forefoot nodes. The starting position is with a barbell placed posterior to the T2 vertebrae and with 20 degree dorsiflexion of the right ankle. A driver is placed on the right ankle creating a plantar flexion, which moves the body vertically upwards until the end point is reached at 10 degree plantarflexion. The barbell's movement is restricted in the global x - and z -directions.

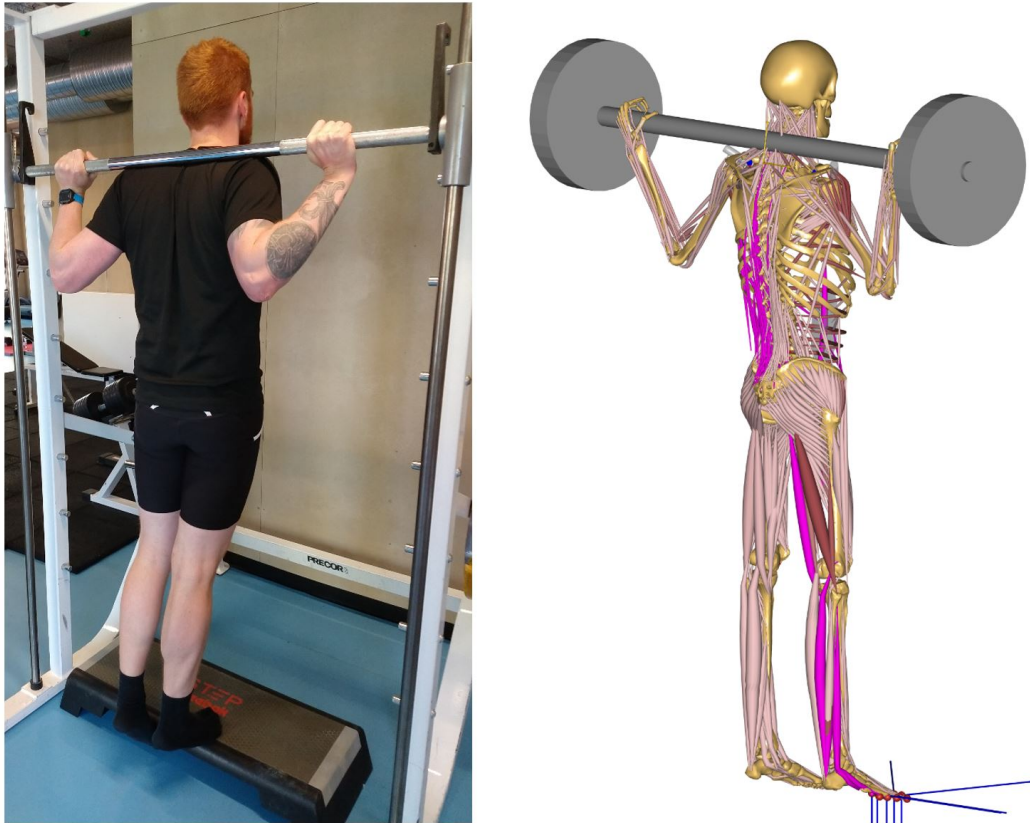


Figure 3: The sticking point position of the calf raise exercise as seen in the fitness center and in the AnyBody Modeling System.

1.5.4. Crunches

The starting position of this model simulates a person supine on the ground with the knees bend at 90 degrees. The feet are locked in place by two drivers; one that restricts the ankle flexion, and one that locks the position of the feet in the GCS, simulating the toes placed under a rack. Further, reaction forces are placed on the pelvis only allowing rotation around the global z -axis. The model has the arms crossed across the chest. A mass is added to represent the mass of the weight plate lying on the chest and is connected through a contact node on the anterior side of the thorax. First, a flexion of the neck occurs and shortly after a lumbar and thorax flexion follows. A driver is placed to rotate the pelvis around the global z -axis -8 degrees each second. Further, a driver is placed on the thorax segment which creates the thorax extension. The combination of these two drivers creates the motion that moves the upperbody off of the ground. The end point of the movement is when the participants is almost sitting up.

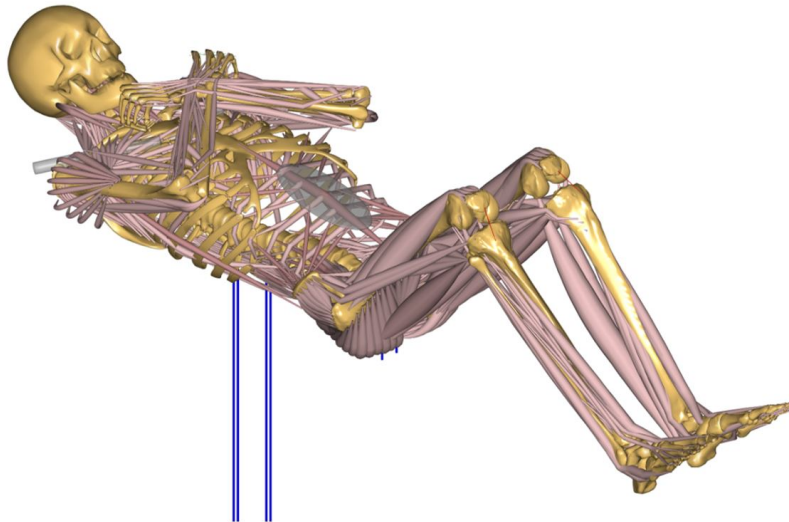


Figure 4: The sticking point position of the crunches exercise as seen in the fitness center and in the AnyBody Modeling System.

1.5.5. Glute bridge

This model simulates a person supine on the floor with 140 degree knee flexion and the feet on the ground. This is achieved by implementing the GRFP class and a driver that ensures that the feet will not move. A barbell is modeled and is placed anteriorly on the hips, by connecting two nodes, one on the bar and one on the pelvis. Further, the skull segment have reaction forces added in the global x - and y -axis simulating the head in contact with the ground. Similar reaction forces are applied to the posterior side of the thorax segment around the scapula in x and y directions. The movement is started by a hip extension driver on each hip, which moves the gluteus muscles off of the ground and ends when there is a straight line from the shoulders through the torso and thighs to the knees. Another driver creates 10 degree neck flexion each second, in order to keep the skull segment on the ground during the movement.

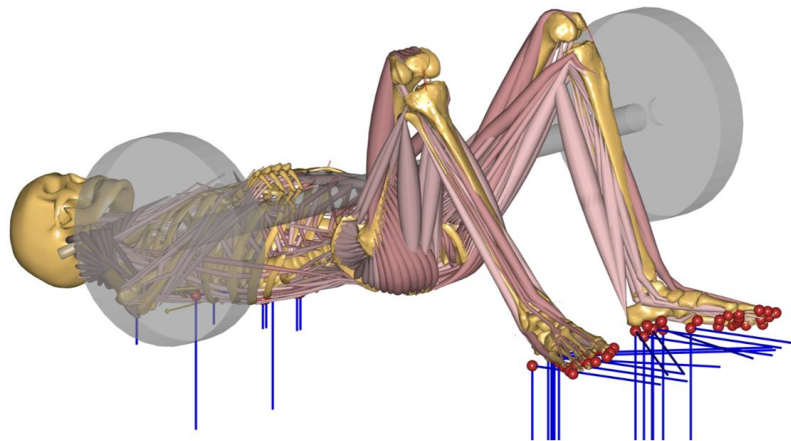


Figure 5: The sticking point position of the glute bridge exercise as seen in the fitness center and in the AnyBody Modeling System.

1.5.6. Hip abduction

The model simulates a person standing on the left leg, with a cable connected to the right ankle. The simulated cable resistance is created using an applied force connected to a node on the shank. The start position is with the right foot slightly (5 degree right hip adduction) crossed in front of the left foot (0 degree left hip adduction). The left foot is locked to the ground achieved by implementing the GRFP class and a driver on the left foot, which ensures that it will not move. The upper body rotation is fixed, to ensure no movement. While keeping the legs straight, a driver abduct the right hip towards the endpoint at 35 degrees abduction. Another driver abduct the left hip slightly, 5 degrees every second, which rotates the pelvis in order to keep the balance of the model.

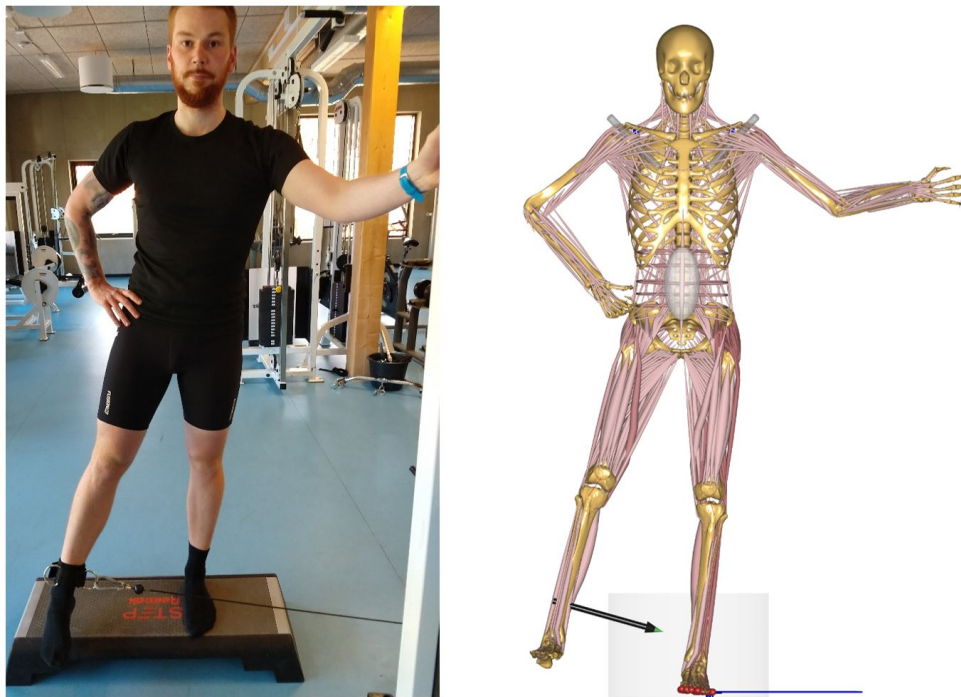


Figure 6: The sticking point position of the hip abduction exercise as seen in the fitness center and in the AnyBody Modeling System.

1.5.7. Hip adduction

The model simulates a person standing on the left leg, with a cable connected to the right ankle. The simulated cable resistance is created using an applied force connected to a node on the shank. The start position is with a 25 degree abduction in the right hip, an abduction of the left hip (15 degree) and a rotation of the pelvis segment around the global x -axis to ensure the model starts in the desired position. The left foot is locked to the ground, achieved by implementing the GRFP class and a driver that ensures that the left foot will not move. The upper body rotation is fixed, to ensure no movement. While keeping the legs straight, a driver adduct the right toward the endpoint at 5 degrees adduction. Another driver adduct the left hip slightly, 5 degrees every second, to keep the balance of the model.

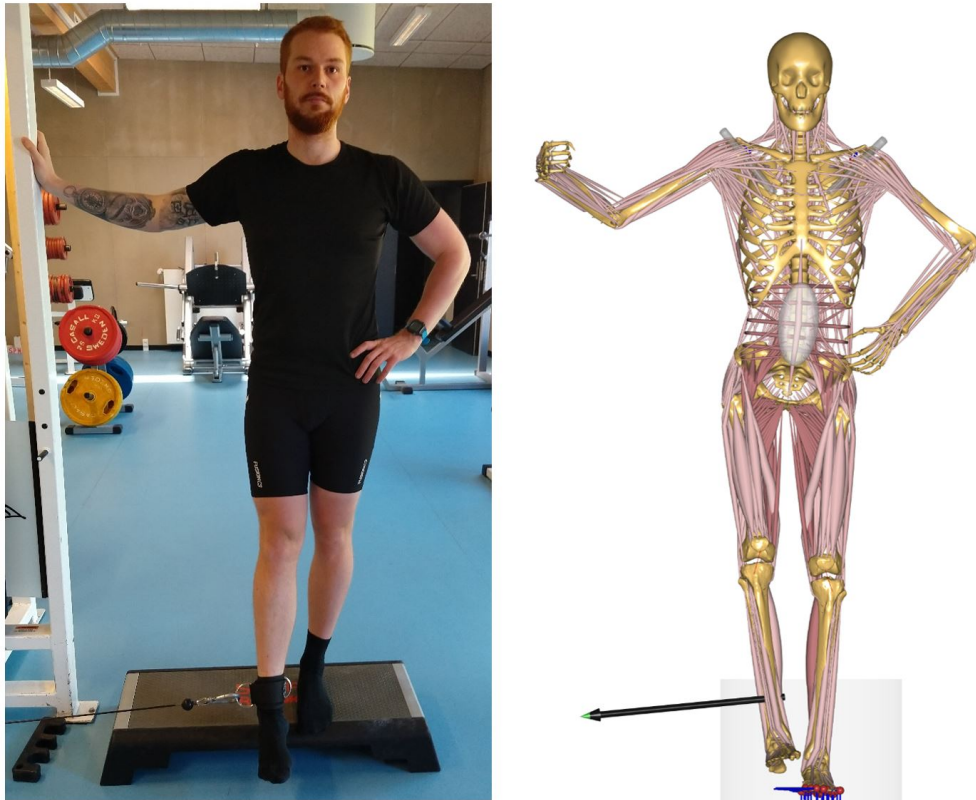


Figure 7: The sticking point position of the hip adduction exercise as seen in the fitness center and in the AnyBody Modeling System.

1.5.8. Horizontal row

The model simulates a person sitting on a bench, where added reaction forces on the pelvis segment restrict movement in global x - and y directions (forward and upward, respectively). Further, both feet is connected to the footrests by the GRFP class. The starting position is with the arms stretched out in front of the body with both hands coupled with a handle through spherical joints. The hands are placed with a distance of 60 cm from each other. The mass of the handle is 4.8 kg and a constant force was added to simulate the cable pulling away from the body. The start position is defined as:

$$handle_{pos0} = |wrist_x| - 0.05 \quad (3)$$

where $wrist_x$ is the x coordinate of the wrist joint in global coordinates, and the constant -0.05 [m] ensures that the elbow joint does not overextend. The movement ends with the handle right in front of the thorax segment near the sternum.

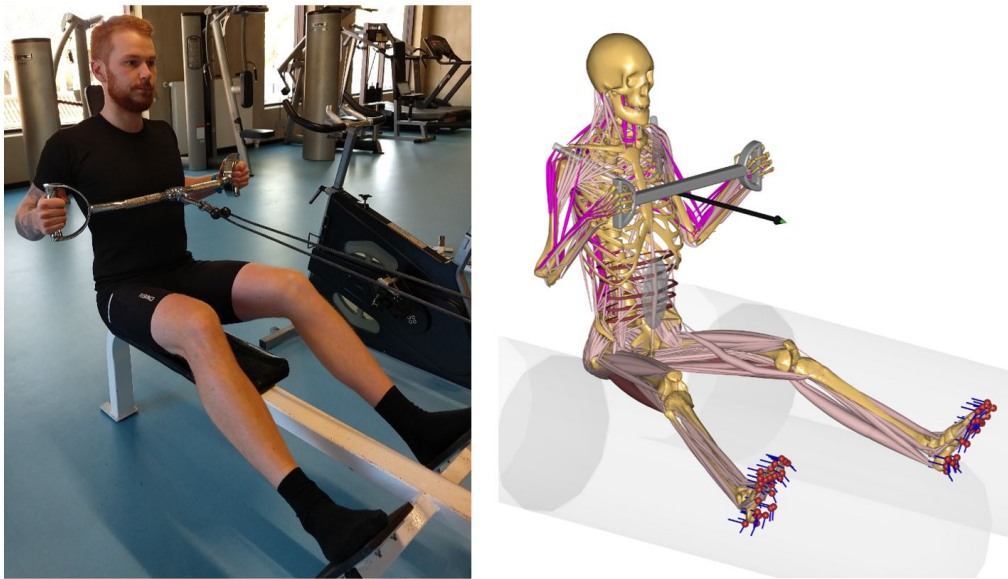


Figure 8: The sticking point position of the horizontal row exercise as seen in the fitness center and in the AnyBody Modeling System.

1.5.9. Hyperextension

The model simulates a person bending forward over a roman chair, resulting in a 75 degree flexion in the hips. A reaction force is applied to the hips, simulating the pad the roman chair pad. The feet are locked in position by creating spherical joints between the heel pad and the heel. Additionally, a segment is modeled to simulate the weight plate held in folded arms anteriorly to the thorax segment. The first driver is placed on the thorax segment simulating the extension of the spine, by 10 degrees each second. The second driver is placed on the hips working to extend the hips 25 degrees each second. At the end of the movement there is a straight line from head to feet.



Figure 9: The sticking point position of the hyperextension exercise as seen in the fitness center and in the AnyBody Modeling System.

1.5.10. Lateral pulldown

The model simulates a person seated on a machine chair and vertically pulling down a handle attached to a cable. The handle is coupled with the carpal segment through a spherical joint. The GRFP class is applied to the feet. Further, reaction forces is added to the pelvis, restricting movement in the global x and y directions. The movement starts with the model's right arm stretched out above the head, with only a slight elbow flexion, and grabbing the handle. The start position of the movement is defined as:

$$handle_{pos0} = (wrist_y 0.8) - 0.6 \quad (4)$$

where $wrist_y$ is the y coordinate of the wrist joint in global coordinates, and the constant -0.6 [m] ensures that the scapula is not elevated beyond its ROM. The movement stops when the wrist is at shoulder height.

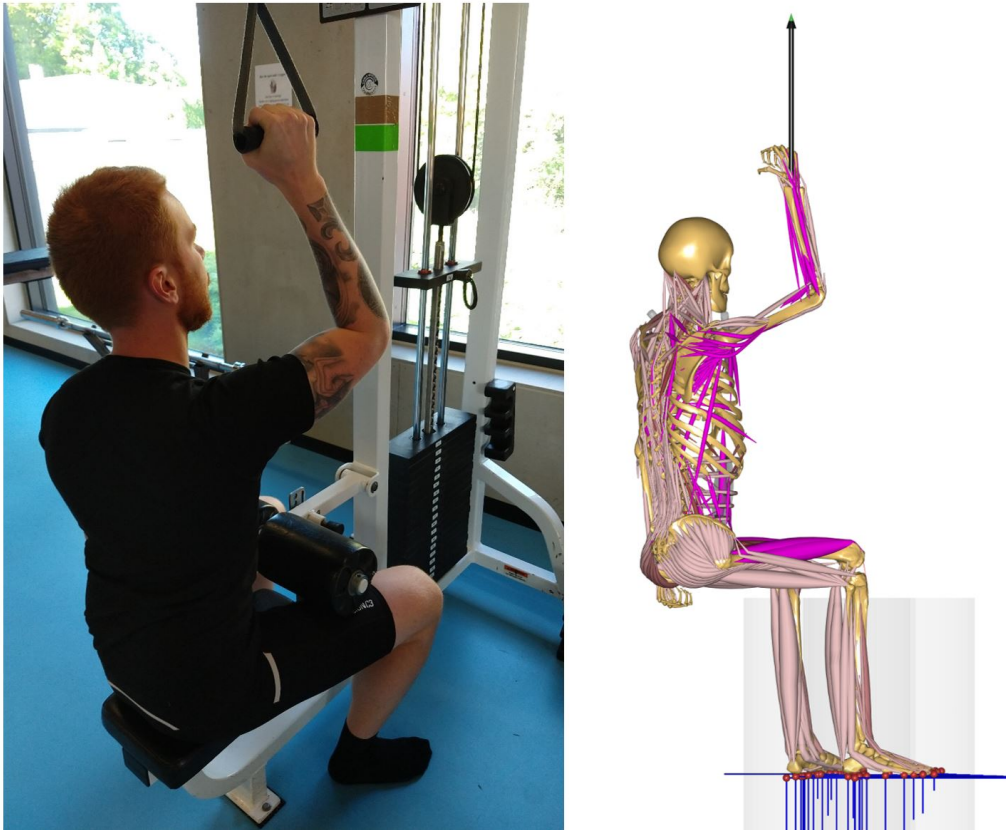


Figure 10: The sticking point position of the lateral pulldown exercise as seen in the fitness center and in the AnyBody Modeling System.

1.5.11. Lateral raise

The model simulates a person standing in an upright position with the back against a wall. The contact between the wall and the back is modeled using the *ContactSurfaceLinPush* class. Further, the GRFP class is added to the feet. The start position is with the right arm stretched down the side and a dumbbell in the hand, coupled through a spherical joint. Then, by an abduction of the shoulder, the hand creates a circular movement upwards, that stops when the hand is in line with the shoulder. The arm is kept stretched throughout the whole movement, abducting 29.5 degrees per second.

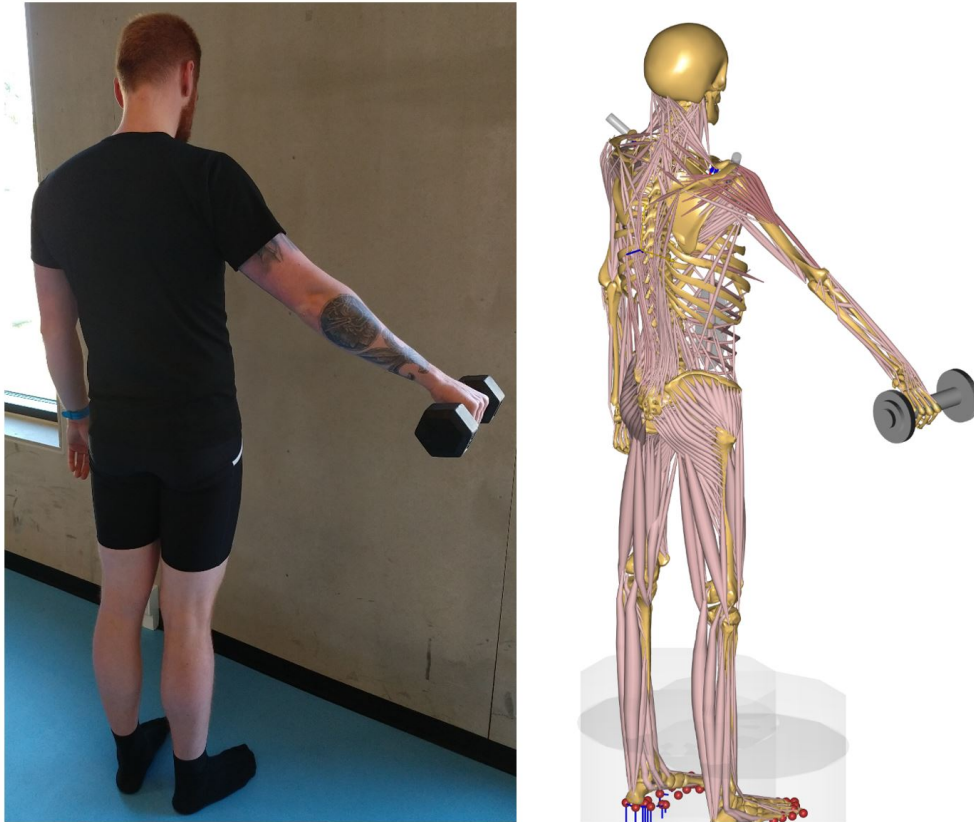


Figure 11: The sticking point position of the lateral raise exercise as seen in the fitness center and in the AnyBody Modeling System.

1.5.12. Leg curl

This model simulates a person in a prone position on a bench, modeled by vertical reaction forces placed on the thorax and thigh segments. Further, reaction forces in all directions are applied to the pelvis, to alleviate movement. The legs are placed in an outstretched position with a machine pad resting on the back side of the right shank around the achilles tendon. An applied force simulating the resistance from the machine pad is added to the heel. The start position is with 25 degree hip flexion and 5 degree knee flexion. A driver is placed at the right knee joint creating 40 degrees of flexion every second.

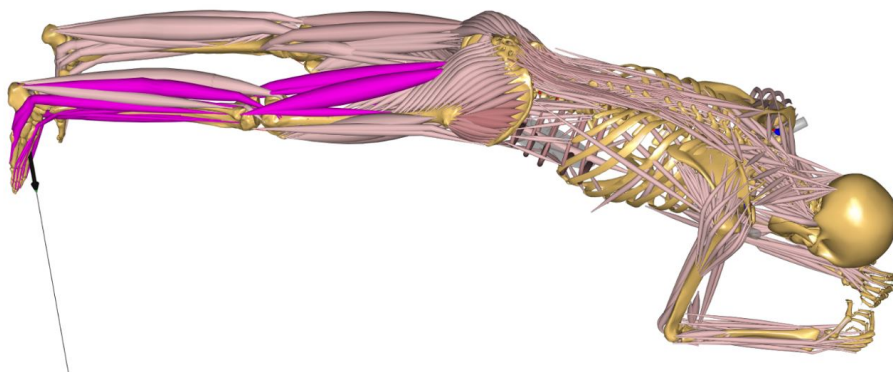


Figure 12: The sticking point position of the leg curl exercise as seen in the fitness center and in the AnyBody Modeling System.

1.5.13. Leg extension

This model simulates a person sitting in a chair, where the back is leaned against a backrest, and the seat have a slight incline (~ 15 degrees). The contact between the back and the backrest is modeled by adding a horizontal reaction force to the thorax segment. Further, reaction forces are applied to the pelvis in all directions, which simulates that the pelvis is stabilized during the movement. The model is sitting in the chair with 80 degree hip flexion, 95 degree knee flexion, and a pad placed on the anterior part of the shank, near the ankles. An applied force, simulating the resistance from the machine pad, is added to the shank. In order to simulate the movement, a driver is placed on the knee joint, extending the knee 30 degrees each second, until the leg is stretched.



Figure 13: The sticking point position of the leg extension exercise as seen in the fitness center and in the AnyBody Modeling System.

1.5.14. Side bends

The model simulates a person standing in an upright position with the back against a wall. The *ContactSurfaceLinPush* class was implemented between the thorax and wall. Further, the GRFP class is added to the feet. The model is starting with the left arm stretched down the side of the body, grabbing a dumbbell, coupled to the hand through a spherical joint. The movement starts with the spine laterally flexed to the left so the dumbbell is at the height of the lower part of the thigh. A driver is applied to the thorax segment in order to laterally extend the spine to the right with 10 degrees each second. Further, in order to allow the left arm to move up along the body, a driver is applied to adduct the shoulder 5 degrees each second. The movement ends when the model is standing upright and the dumbbell is at the height of the left hip.



Figure 14: The sticking point position of the side bends exercise as seen in the fitness center and in the AnyBody Modeling System.

1.5.15. Triceps extension

The model simulates a person standing with the back against a wall, simulated *ContactSurfaceLinPush* class. The model starts with the right hand grabbing the handle, simulated by a spherical joint between the two. The mass of the handle is set to 0.10 kg, to represent the actual mass of the handle from the fitness center. The pull force from the cable is represented by a force working vertically downwards in the GCS. A driver is added to the right elbow joint, starting the movement at 120 degree elbow flexion and extending the elbow by 35 degrees every second.

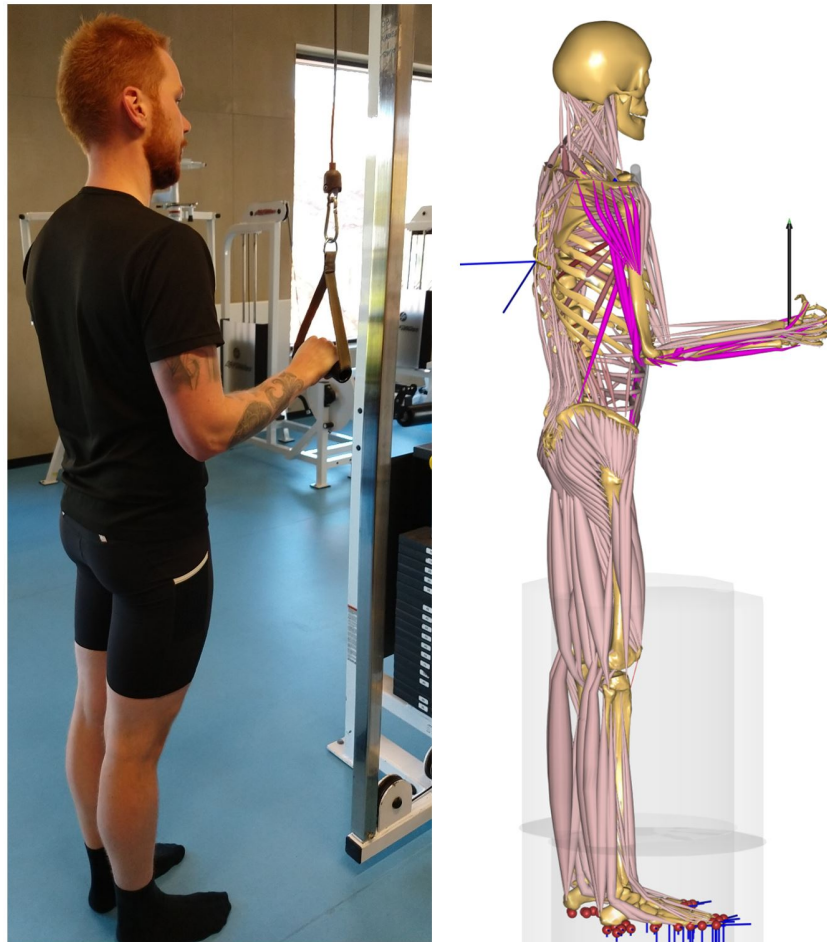


Figure 15: The sticking point position of the triceps extension exercise as seen in the fitness center and in the AnyBody Modeling System.

1.6. Models for part 2

For part 2 of the present study, the built-in AMS *EvaluateJointStrength* study class was used to estimate the maximum joint torques of the standard scaled strength scaled (LMF_{SS}) and the optimization based strength-scaled (OPT_{SS}) subject-specific models, respectively. The study excludes the parts of the body not needed for the analysis and fixes the upperbody using reaction forces. Furthermore, it fixes the joint in question in the desired position and adds constraints to all the other degrees of freedom in the model. It applies a force (F) at the measured joint and calculates the joint torque (T) as; $T = \frac{F}{a+0.00000001}$, where a is the maximum muscle activity. In order to do this calculation, the study implements the min/max muscle recruitment criterion making the relationship between F and a linear [10]. The present study evaluated the peak joint torque (PJT) for the sticking point position for the five tested movements (i.e. ankle plantar flexion, knee and elbow flexion and extension), in-line with the positions used in part 1.

1.6.1. Comparing joint torques

Originally the present study aimed at comparing the measured mean PJT from the dynamometer tests with the AMS PJT across the five movements. During the analysis, the AMS PJT showed unrealistic values for the ankle plantar flexion, and knee flexion and extension movements. The results for one participant (p_{01}) are shown in table 1. To understand this discrepancy, the *EvaluateJointStrength* study covering a full ROM of the movements were investigated (figure 16). Ideally these graphs should approximate a bell curve, much like the standard graph of the force-length relationship. Clearly, this is not the case for the knee extension movement. The present study implemented the AMS simple muscle models, characterized by only having a nominal strength parameter, based on the force output at optimal fiber length. Considering the use of these muscle models, it was theorized that the combination of simple muscle models and testing angles near end ROM resulted in a large overestimation of joint torque for the AMS models. Furthermore, for all five movements the 3-element Hill-type (3E) muscle models was implemented to see if the inclusion of a force-length and force-velocity relationship could improve the results. Table 1 shows that using the 3E muscle models alleviate much of the discrepancy between measured and estimated PJT. This could indicate that caution should be taken when utilizing the simple muscle models in comparison with dynamometer obtained PJT.

Table 1: Peak joint torque [Nm] for the dynamometer experiment (DYNO), using either simple muscle models applying the standard scaled (LMF_{SS}) or optimization based (OPT_{SS}), or the 3-element Hill-type ($3E$) muscle models. Ankle plantar flexion is denoted as ankle flexion.

	Ankle flexion	Elbow flexion	Elbow extension	Knee flexion	Knee extension
Joint angle [°]	-14	30	73	5	5
<i>DYNO</i>	211.0	62.3	68.6	99.8	180.8
<i>LMF_{SS}</i>	523.9	76.1	76.6	306.3	1244.5
<i>OPT_{SS}</i>	518.8	57.4	58.7	351.5	1244.6
<i>3E</i>	685.1	32.1	21.7	528.4	332.8

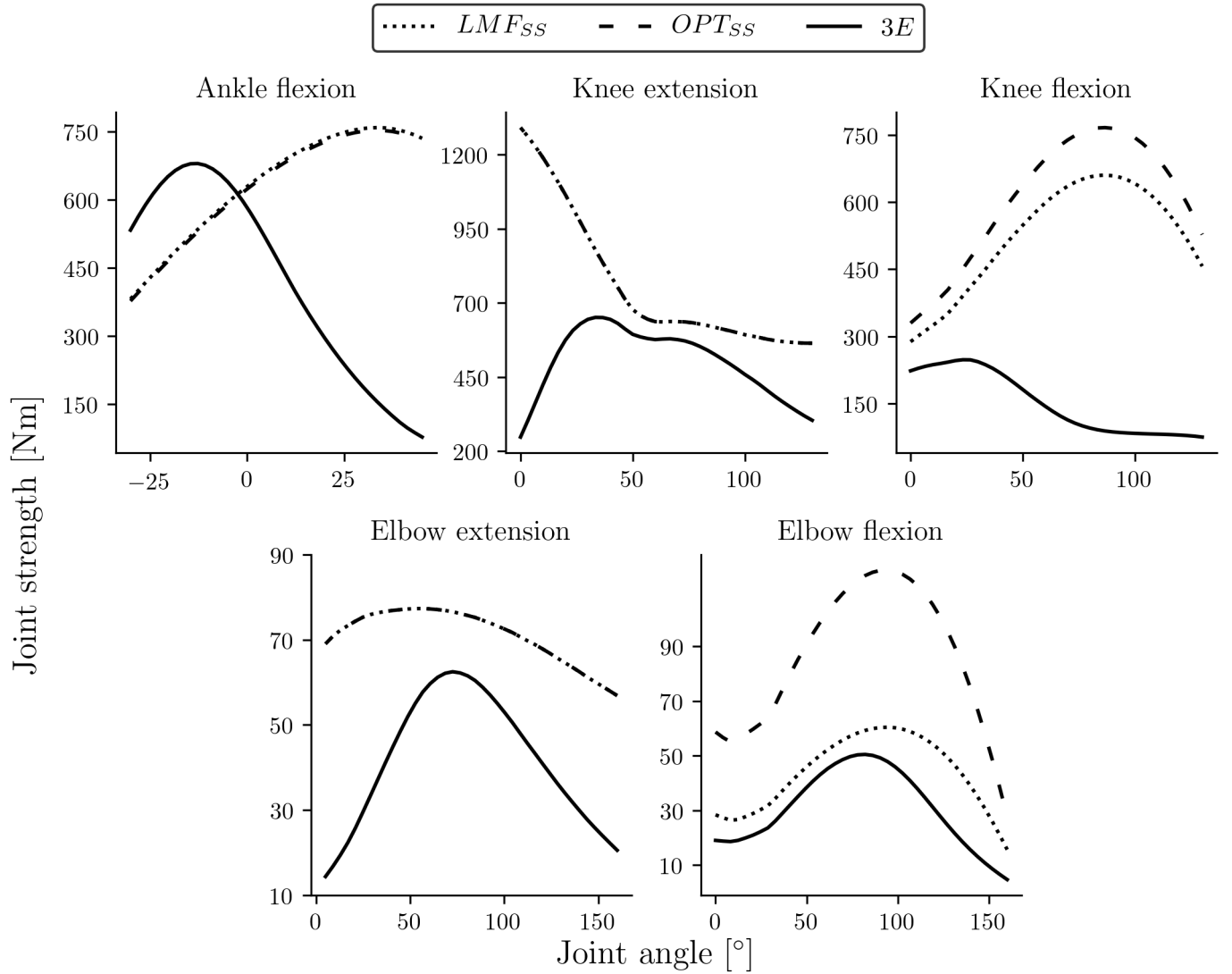


Figure 16: Relationship between joint strength [Nm] and joint angle [°] for one participant (p_{01}) using either the simple muscle models, with the standard scaled strength-scaling (LMF_{SS}) or the optimization based strength-scaling (OPT_{SS}), or the 3-element Hill-type (3E) muscle models. Each subplot represents one of the five movements tested in the validation experiment.

2. Subject-specific geometric scaling

The purpose of this worksheet is to introduce different methods in order to geometrically scale musculoskeletal models in the AMS. Further, this worksheet will show two standard methods available in the AMS to scale the strength of said models.

In order to scale musculoskeletal models, the AMS have the capability to implement different scaling laws depending on the amount of subject-specific anthropometric information available. The unscaled AMS model is created with a stature of 1.8 m and a mass of 75 kg, based on a multitude of cadaver studies [3–6]. The simplest scaling law is the *standard scaling law*, where the model is scaled in accordance with the 50th percentile European male anthropometrics. This method is mostly used when no subject-specific information is available. However, when external measures, such as body mass and stature is known, the *uniform scaling law* is more preferred for creating subject-specific models. This method scales the segments linearly in all directions, based on proportions of the total subject stature, relative to the stature of the unscaled model, as defined by Rasmussen et al. [11]:

$$s = \mathbf{S}p + t \quad (5)$$

where s represents the scaled node's position vector in its local coordinate system, p is the positional vector of the unscaled node, and t represent a translational vector of the segments local coordinate system onto the scaled segment. \mathbf{S} is a 3×3 diagonal scaling matrix, given by:

$$\mathbf{S} = \begin{bmatrix} k_x & & \\ & k_y & \\ & & k_z \end{bmatrix} \quad (6)$$

where k is the scaling factor. For the *uniform scaling law* $k_x = k_y = k_z$. A more advanced geometrical scaling method is the *XYZ scaling law*, which uses segment specific dimensions to scale the model in all three dimensions of the segments local coordinate system. This is achieved by changing the scale factors k in the scaling matrix \mathbf{S} , in accordance with the actual segment dimensions of the subject.

The muscle strength in the *uniform scaling law* is scaled through a non-linear regression with the power of $\frac{2}{3}$.

$$f = \left(\frac{m_{s0}}{m_{s1}} \right)^{\frac{2}{3}} \quad (7)$$

where m_{s0} is the estimated mass of the individual segment based on the segment's mass percentage of the total body mass [12]. m_{s1} is the standard mass from the cadaver based models used in the unscaled model in AMS. A disadvantage of the *uniform scaling law* is the inability to account for BMI and body fat-percentage (R_{fat}), why it often underestimates the muscle strength for tall light subjects and overestimates for short heavy subjects. In order to overcome this problem the *Length-Mass-Fat (LMF) scaling law*, can be implemented to scale the muscle strength [11]. This method is feasible with the same anthropometric information as the *uniform scaling law*, however, it also takes the fat-percentage into account by calculating how large a proportion of the total body mass is muscles, fat, and other (e.g. bone, tissue, ligaments); $R_{muscles} = 1 - R_{fat} - R_{other}$, where R_{other} is set to 50% in the AMS, and R_{fat} is the fat-percentage found by a regression equation relating BMI to fat-percentage, as defined by Frankenfield et al. [13]:

$$\text{Men: } R_{fat} = -0.09 + 0.0149BMI - 0.00009BMI^2 \quad (8a)$$

$$\text{Women: } R_{fat} = -0.08 + 0.0203BMI - 0.000156BMI^2 \quad (8b)$$

The initial muscle strength can then be calculated as:

$$f = f_0 \frac{k_m R_{muscle1}}{k_L R_{muscle0}} \quad (9)$$

where f_0 is the nominal strength of the unscaled segment, k_m and k_L are the mass and length ratios between the unscaled segment (denoted 0) and the subject-specific segment (denoted 1), respectively.

$$k_m = \frac{m_1}{m_0} \quad (10)$$

$$k_L = \frac{L_1}{L_0} \quad (11)$$

For the subject-specific models in the present study, a combination of the *XYZ* and *LMF scaling laws* were used. The *XYZ scaling law* was used to scale the geometry of the participants and the *LMF scaling law* was used as a standard muscle strength scaling.

2.1. Calculating subject-specific scaling factors

In order to scale a standard AMS model according to subject-specific data, the anthropometric measures from the ANSUR dataset [14], were used to compile a dataset of XYZ scaling factors (k_x , k_y , and k_z) for each of the subjects in the ANSUR dataset, based on a method developed by Andersen et al. [8]. This is achieved by creating a standard human model locked in a standing position using hard drivers on all movements. Further, a subset of ANSUR measures were modeled as kinematic measures with soft drivers. By running a kinematic optimization study (*AnyKinOptStudy*) [8], in one timestep, a kinematic error between the modeled measure and the one from ANSUR was minimized, by allowing the segment dimensions to vary. The length dimension of each segment is scaled according to the ANSUR measures, where the depth and width dimension of each segment is based on a proportion of the total body stature. This entails that subjects with short legs still gets realistic leg dimensions.

Using the compiled dataset as a basic population and the present study’s participant anthropometric measures as primal constraints, a closed-form optimization problem using PCA was solved, to obtain subject-specific scaling factors (k_x , k_y , and k_z) for each participant. The method uses the given primal constraint and tries to keep all other anthropometric dimensions as ordinary as possible, given the information from the ANSUR dataset. The present study anthropometric measures were taken in accordance with the ANSUR dataset [14] and consisted of; acromial height (sitting), acromion-radial length, foot breadth, foot length, handbreadth, hand length, heel breadth, iliocristale height, lateral femoral epicondyle height, lateral malleolus height, radiale-styilion length, and stature. In addition, the body mass, age, and gender were noted for all participants resulting in a total of 15 primal constraints.

3. Defining the sticking point

This worksheet describes the details of the sticking point phenomenon.

When examining dynamic repetitions of strength exercises, the success criteria is often the ability to move a mass through a pre-described ROM. A failed repetition is therefore characterized by the subject being unable to exert the force needed to move a mass throughout the ROM. Previous research has sought to identify the mechanisms and postures where failure occurs in order to develop training schemes and knowledge of how to better overcome this point. Investigating the difference in strength exerted during concentric and eccentric contractions, Hollander et al. [15] identified that eccentric contractions are able to produce more force than concentric contractions. Therefore, failure will occur during the concentric part of a dynamic repetition. Extensive studies have been performed to identify the point during concentric contractions where failure is most likely to occur [1, 16–18]. This point or phenomenon is often noted as a “*sticking point*” or “*sticking region*”, and Kompf and Arandelovic [1] defines it as:

“... the point at which failure occurs when exercise is taken to the point of momentary muscular failure” [1]

If the subject manages to overcome the sticking point, there is a higher possibility of completing the repetition. However, the sticking point possesses a large interpersonal variation, making its location hard to predict without subject-specific data, such as motion capture data of the repetition. A portion of this variation can be related to the large discrepancy in morphology between individuals [1]. Since the present study aimed to develop a workflow involving simple data inputs, it was deemed infeasible to collect subject-specific technique data in order to predict subject-specific sticking points. As previously mentioned, the sticking point is the hardest point to overcome during the ROM, which coincide with the position at which the AMS models have the highest a . Therefore, this timestep was chosen as the sticking point position for that given movement, greatly reducing the convergence time of the optimization routine, since the inverse dynamics analysis would only be computed in this timestep. The joint angles of the model in the sticking point position can be found in table 2.

Table 2: Joint angles [°] for the static positions in each exercise model. GH, SC, and PT denote glenohumeral, sternoclavicular, and pelvisthorax, respectively. Empty cells denote an angle of 0.0.

Posture	Bench press	Biceps curls	Calf raise	Horizontal row	Lateral pull-down	Lateral raise	Leg curl	Leg extension	Side bends	Triceps extension
PelvisPosY	-	0.85	0.9	-	0.5	0.9	-	-	0.9	0.9
PelvisRotZ	85.0	-	0.1	5.0	-	-	-105.0	20.0	-	-
PTLateralBending	-	-	-	-	-	-	-	-	-30.0	-
NeckExtension	20.0	-	-	-	-	-	-	-	-	-
SCProtraction	-17.3	-23.0	-34.1	-41.5	-30.0	-29.0	-31.7	-31.7	-15.7	-13.3
SCElevation	12.3	5.0	4.3	4.7	11.5	11.0	11.6	11.6	4.2	3.1
GHFlexion	-33.8	10.0	-1.8	5.6	117.7	-	85.0	-	-	10.0
GHAbduction	66.5	5.0	43.1	22.0	-2.6	59.9	10.0	10.0	5.0	-
GHEXternalRotation	7.6	0.0	107.1	24.1	-8.5	5.0	-	-	-	-
ElbowFlexion	126.7	29.8	110.2	117.1	62.5	5.0	100.0	-	-	80.2
ElbowPronation	56.7	-75.0	-1.6	-0.3	5.1	30.0	-	-	-	-
WristFlexion	15.0	-	-	-	-	-	-	-	-	-
HipFlexion	-	-	0.8	85.0	90.0	-	25.0	80.0	-	-
HipAbduction	-	5.0	6.3	20.0	10.0	5.0	-	5.0	5.0	5.0
HipExternalRotation	-	-	0.9	-	-	-	-	-	-	-
KneeFlexion	90.0	-	1.3	25.0	90.0	-	5.0	5.1	-	-
AnklePlantarFlexion	-	-	9.5	10.0	-	-	-	-	-	-
SubTalarEverson	-	-	0.2	-	-	-	-	-	-	-

4. Calculating model strength

The following worksheet describes the details for calculating the maximum mass ($\widehat{1RM}$) that the exercise models are able to sustain in a static posture.

The assumptions regarding the calculation are based on the selected muscle recruitment criterion. The present study applied the min/max muscle recruitment criterion [10], where the load is distributed across all available muscles in order to minimize the maximum relative muscle force, which is denoted as a . This muscle recruitment criterion is suitable for scenarios where maximum strength is desired, since the criterion can be thought of as a postponement of fatigue. As noted by Rasmussen et al. [10], the min/max criterion shows a linear development between the muscle force and the external moment. For the present study the relationship between the a and the external applied mass (m) [kg] was investigated, and

figure 17 shows that the same linear development can be seen for applied masses above a given threshold. This is an important characteristic as it simplifies the calculation of which mass will result in $a = 1$. The assumed linear relationship can be characterized by:

$$a = \alpha * m + \beta \quad (12)$$

where β is the y -axis intercept. The slope (α) can be calculated using the coordinates of two points along one of the graphs in figure 17.

$$\alpha = \frac{a_2 - a_1}{m_2 - m_1} \quad (13)$$

Subsequently, knowing that one coordinate for the $\widehat{1RM}$ is $a = 1$, equation 13 can be rearranged into

$$\widehat{1RM} = \frac{1}{\alpha} - \frac{a}{\alpha} + m \quad (14)$$

where $\widehat{1RM}$ is the maximum applicable mass. As an example of the calculation, the $\widehat{1RM}$ of each exercise for one participant (p_{01}) was calculated using equation 13 and 14. Table 3 shows the results for the calculated $\widehat{1RM}$ and the a when applying $\widehat{1RM}$ and running the inverse dynamics analysis.

Table 3: An example of $\widehat{1RM}$ calculation and corresponding maximum muscle activity (a) for the 10 included exercises, for one participant (p_{01}).

Exercise	$\widehat{1RM}$	a
Bench press	84.0845	1
Biceps curl	15.3224	1
Calf raise	55.4994	1
Horizontal row	57.6782	1
Lateral pulldown	27.7818	1
Lateral raise	41.9646	1
Leg curl	49.4671	1
Leg extension	55.2014	1
Side bends	30.0198	1
Triceps extension	27.0566	1

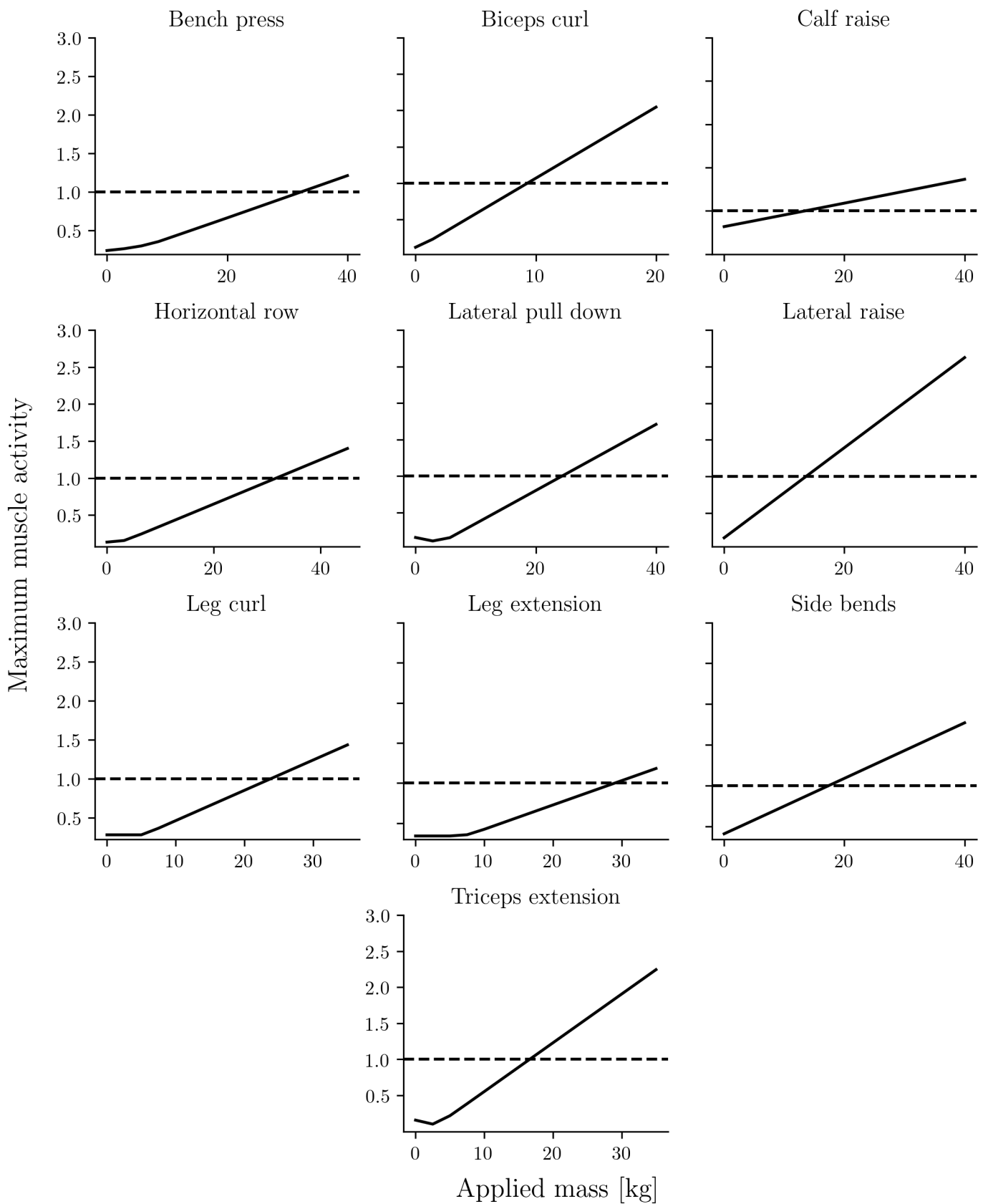


Figure 17: Relationship between applied mass and maximum muscle activity for one participant (p_{01}), for each of the 10 included exercise models. Dashed line indicate a maximum muscle activity of 1.

5. Strength optimization

The following worksheet is submitted to clarify certain details regarding the workflow and settings during the optimization process.

5.1. Introduction

The present study defined a optimization problem, aimed at minimizing an objective function, in order to scale the strength of a set of subject-specific AMS models, to match a field obtained set of 1RM estimations. The general idea was that a design variable (κ) for each exercise could be calculated, thereby creating a problem with a number of design variables equal to the number of included exercises ($n_\kappa = n_{exercises}$). The calculated κ values were used in a linear system of equations to solve for a series of strength factors to be implemented in the AMS models. These strength factors represents the change of each individual muscle strength in the models. It was deemed infeasible to optimize the total number of strength factors, as this would create 918 design variables, opposed to the included 10. The present study implemented a simple objective function:

$$J = \sum_{i=1}^n (\widehat{1RM}_i - 1RM_i)^2 \quad (15)$$

where $\widehat{1RM}$ is the maximum applicable mass of the AMS models, and 1RM is the one-repetition-maximum obtained in the field strength test.

5.2. Dependencies

For the workflow to be practical and ready for others to use, the number of dependent software packages were kept at a minimum, and focus was to use open-source software. For obvious reasons the AMS software is needed as this founds the basis for the musculoskeletal models and inverse dynamics calculations. It further provides a console application, which founds be base for the automatization of model simulations when combined with the AnyPyTools python library [19]. The AMS is the only commercial licensed software used. To set up and perform the optimization itself, the open-source programming language Python 3.7 (Python Software Foundation, Beaverton, Or, USA) was used alongside the free libraries; Numpy [20], Pandas [21], Nlopt [22], and AnyPyTools [23].

5.3. Workflow

As seen in figure 18, the workflow starts by estimating a 1RM measure for each field tested exercise, using a user defined regression formula. Thereafter, the optimizer solves for the strength factors to implement in the AMS models. The $\widehat{1RM}$ is returned to the optimizer in order to evaluate the objective function. After convergence, the new strength factors can be implemented and used to validate the subject-specific models.

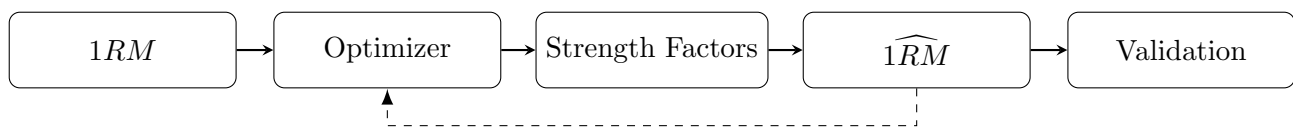


Figure 18: Flowchart of the optimization workflow.

5.4. Optimization algorithm benchmark

The present study did not aim at developing a optimization algorithm, instead a practical evaluation of already existing algorithms was performed. The evaluation aimed at benchmarking available algorithms to investigate their performance and suitability for the strength optimization problem. Benchmark parameters included; objective function value (J), time to convergence (TTC), and number of objective function evaluations (nEval) across two participants' (p_{03} , p_{12}) field obtained data. The tested algorithms were chosen based on their

description in the Nlopt Python library. The library group algorithms by their conditions and suitability. The present study involved an unconstrained minimization problem. Further, no derivative information was available for the optimizer, why only derivative free algorithms were benchmarked. The Nlopt library offers six algorithms suited for unconstrained non-derivative optimization. The present study implemented the NEWUOA BOUND algorithm [24], based on the algorithm evaluation.

5.5. Omitting the optimization

Concurrent to developing the optimization workflow, a strength-scaling method using only a system of linear equations (SLE_{SS}), to solve for the desired strength factors, was explored. The method would have the potential to eliminate the need of an optimizer iteratively finding the κ values to solve for the strength factors for the AMS models. By assuming that the change in strength could be linearly approximated, a system of linear equations could be formed to solve in a matter of seconds, instead of hours using the optimizer. A working method based on these assumptions could prove to be much more practical for users of musculoskeletal models, as the complexity is lowered. The present study tested the following system:

$$\mathbf{A}diag(f_0)\mathbf{B} = 1\widehat{RM} - 1RM \quad (16)$$

where \mathbf{B} is a matrix of principal components of \mathbf{A} and \mathbf{A} is a sensitivity measure formed by

$$\mathbf{A}_{i,j} = \sum_j^n \frac{\Delta 1\widehat{RM}_i}{\Delta f_i} \quad (17)$$

where $1\widehat{RM}_i$ is the maximum permissible mass that the model can move and f_i is the nominal strength of the i^{th} muscle over the j^{th} exercise. This system was solved for each of the 28 participants and their normalized root mean square error (NRMSE) was evaluated to assess the accuracy (table 4). The table shows that the system is effective in lowering the NRMSE for all participants. More interesting is the fact that participant 04, 07, 12, 15, 17, 25, and 27 shows a lower NRMSE for the SLE_{SS} , when compared to the OPT_{SS} . This could indicate that the optimization algorithm might have been stuck in the process of determining the strength, or that the termination criteria, based on how much the objective function changes from iteration to iteration, have been set to high. This entails that further research investigating how the optimization problem behave, and if other types of optimization algorithms are needed, to converge to a global minimum.

The time needed to solve the equation system in order to obtain the desired strength factors in the AMS models, by far outperform the optimization routine. For one participant (p_{02}), the optimization routine converged after ~ 2 hours, whereas the equation system was solved in a matter of seconds, resulting in almost the same accuracy (table 4). This is intriguing as it provides hope that further research can improve the equation system, in order to have a fast and reliable method of performing strength-scaling. Researches and other users of musculoskeletal models could either apply the equation system, to obtain a better than standard result, or implement the more time consuming optimization routine, to gain further accuracy based on the accuracy needs.

Table 4: Results of scaling the AnyBody Modeling System models' strength, based on a linear system of equations. The normalized root mean square error (NRMSE) of the standard scaled (LMF_{SS}), the optimization based (OPT_{SS}), and the system of linear equations (SLE_{SS}) conditions are shown for each participant across all exercises.

Participant	NRMSE <i>LMF_{SS}</i>	NRMSE <i>OPT_{SS}</i>	NRMSE <i>SLE_{SS}</i>
<i>p</i> ₀₁	56.44	17.87	35.10
<i>p</i> ₀₂	62.38	42.82	43.76
<i>p</i> ₀₃	73.83	36.31	58.96
<i>p</i> ₀₄	43.68	47.24	28.14
<i>p</i> ₀₅	40.99	21.91	28.16
<i>p</i> ₀₆	48.09	24.35	37.97
<i>p</i> ₀₇	51.07	47.31	36.86
<i>p</i> ₀₈	79.75	34.25	47.64
<i>p</i> ₀₉	59.85	31.39	41.36
<i>p</i> ₁₀	51.80	10.58	35.64
<i>p</i> ₁₁	49.15	28.05	34.47
<i>p</i> ₁₂	44.99	33.62	33.52
<i>p</i> ₁₃	67.68	40.82	51.63
<i>p</i> ₁₄	60.94	42.45	45.17
<i>p</i> ₁₅	59.18	49.63	41.36
<i>p</i> ₁₆	53.78	23.12	41.40
<i>p</i> ₁₇	47.98	38.21	32.22
<i>p</i> ₁₈	46.78	5.35	32.60
<i>p</i> ₁₉	39.72	8.87	27.32
<i>p</i> ₂₀	52.99	24.02	40.87
<i>p</i> ₂₁	47.61	22.52	30.62
<i>p</i> ₂₂	46.49	11.41	32.11
<i>p</i> ₂₃	45.13	12.43	27.35
<i>p</i> ₂₄	39.32	16.57	28.12
<i>p</i> ₂₅	52.63	45.04	36.59
<i>p</i> ₂₆	44.07	16.87	28.33
<i>p</i> ₂₇	52.92	52.27	33.36
<i>p</i> ₂₈	41.04	16.24	28.51
Mean	52.15	28.63	36.40
SD	10.03	13.93	7.93

5.5.1. More iterations

An iterative process of updating the equation system was investigated. A fully updated system would require the \mathbf{A} matrix to be recalculated after each iteration, as the new strength factors would alter the sensitivity of the muscles. Calculating the \mathbf{A} matrix is the costliest term in equation 16, and an assumption was made to only update the non-expensive term, $1RM$. The resulting κ values was used to solve for a set of strength factors, to implement in the AMS models. This resulted in an updated $1RM$, which could be implemented in the equation system, to create new κ values. This process was repeated for five iterations, for two participants data, in order to see if the accuracy in terms of NRMSE values between the SLE_{SS} and the field obtained $1RM$ could be lowered (table 5). As seen in table 5, using multiple iterations of the equation system, only updating the $1RM$ term, does not improve the NRMSE after the first iteration. Instead the NRMSE toggle up and down further from the results obtained in the first iteration.

Table 5: Normalized root mean square error (NRMSE) across all exercises for each system of linear equation strength-scaling (SLE_{SS}) iteration, for participant p_{01} and p_{02} , respectively.

Participant	Iteration	1	2	3	4	5
p_{01}		35.1	42.3	40.6	41.1	41.0
p_{02}		43.8	50.8	48.4	49.3	48.9

6. Protocol specific details

The first part of this worksheet will describe the gearing assessment of the strength exercise machines. The second part documents details, assumptions and limitations related to the field test during part 1.

For many regular strength exercise machines, there is some sort of gearing. The gearing controls the exchange ratio between the applied mass from the weight stack, and the actual force required to move the mass throughout a prescribed ROM. The present study estimated the gearing of the strength exercise machines used during the field test. These included a prone leg curl, a leg extension, a horizontal row, and a lateral pulldown machine, and a cable tower. Further, the smith rack used was measured in order to apply the accurate mass of the embedded barbell to the calf raise exercise. To estimate any possible exchange ratio, a handheld analogue ring dynamometer (Tiedemann Instruments GmbH & Co. KG, Garmisch-Partenkirchen, Germany) was used to measure the force required to move the machine handle. To ensure that any irregularity was caught, the section of the weight stack measured corresponded to the range used during the field test. Further, all machines were tested within the full ROM of the given exercise for each machine, ensuring that peak forces needed during the exercise was measured. A table relating measured μm to kg was given by the dynamometer manufacturer, which was used to calculate the following linear regression equation:

$$m = 1.8337d \tag{18}$$

where m is the mass [kg] of the weight stack and d is the measured μm from the dynamometer. The actual mass moved after accounting for the gearing, was found by multiplying the μm by 1.8337. This resulted in a series of data showing the exchange ratio between the mass of the weight stack and the actual mass moved. The discrepancies between these two is an important factor, because the AMS models do not have any gearing implemented and/or accounted for. A mean peak displacement of three peak force measurements per weight stack increment was used to plot this relationship. Figure 19 shows that the relationship is linear for all five machines ($R^2 > 0.95$). Therefore, the participants' recorded moved mass was multiplied by a coefficient corresponding to the regression coefficient found for each strength exercise machine.

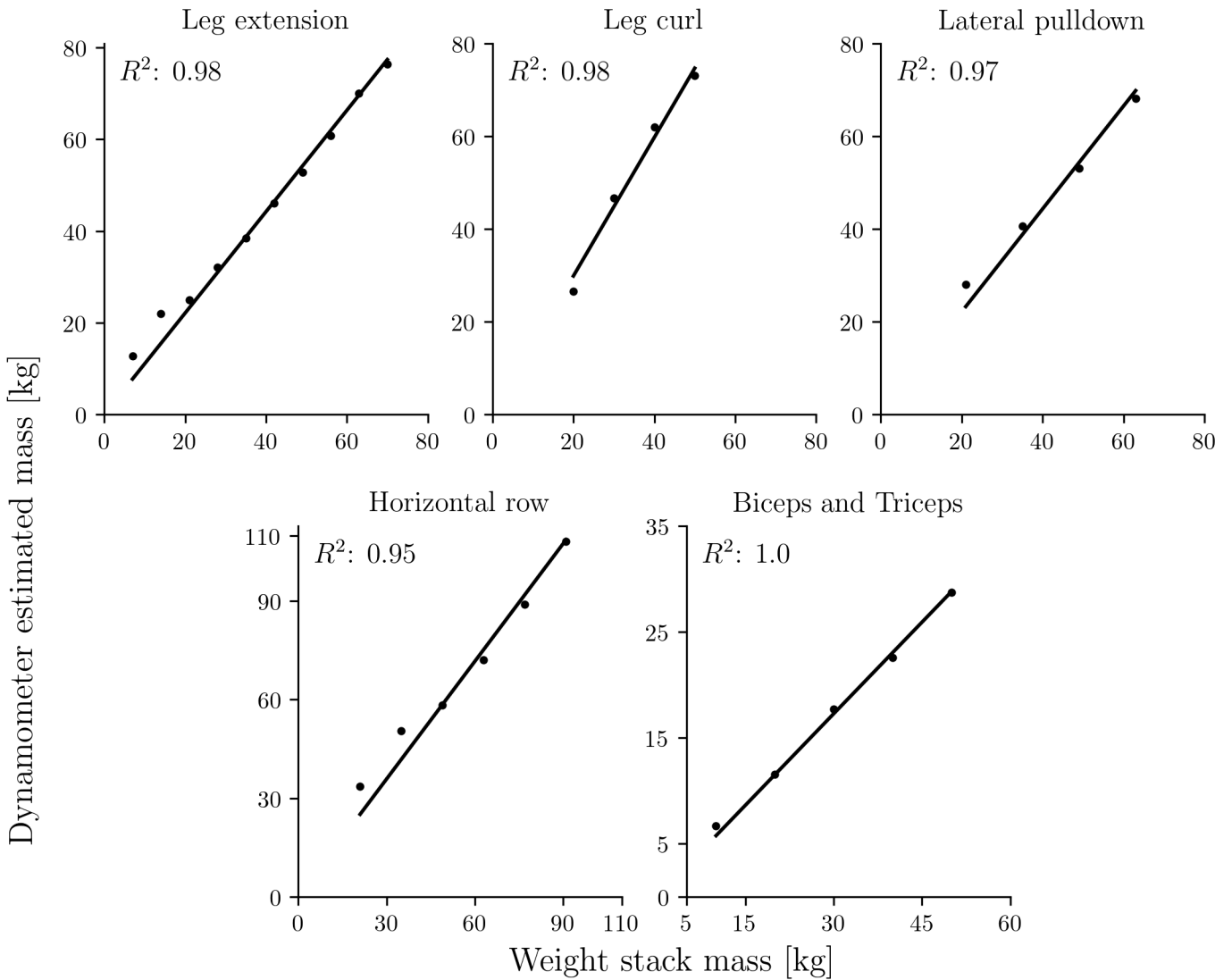


Figure 19: The relationship between weight stack mass and estimated mass, based on dynamometer displacement, for each of the used exercise machines. the coefficient of determination is denoted as R^2 .

6.1. Fitness equipment

One goal of the field test was to use simple equipment and exercises when possible, including a standard measuring tape to measure stature and body dimensions, and a platform scale (EOE 150K50L, Kern & Sohn GmbH, Balingen, Germany) to measure body mass. General equipment found in an average fitness center were used, and included; barbells (5 kg, 15 kg, 20 kg), weight plates (1.25 kg, 2.5 kg, 5 kg, 10 kg, 15 kg, 20 kg, 25 kg), dumbbells (1 kg - 55 kg), cable tower, sitting leg extension machine, prone leg curl machine, cable lateral pulldown machine, and a seated horizontal row machine.

Although effort was put in to implement simple equipment, limitations occurred during testing. For the side bends exercise, a grip strap was needed to ensure that the participants were not limited by their grip strength, since this failure criteria could be seen in the pilot test. Furthermore, several of the moderate experienced participants (i.e. one participant with two years of experience and five participants with five years of experience) were able to lift the heaviest dumbbell (55 kg) more than seven times. An alternative setup could have been implemented utilizing the smith rack, however, it was found an infeasible setup, since it did

not follow the same exercise technique. This limitation negatively affected the participants 1RM estimation for the given exercise.

For the crunches exercise, several participants experienced discomfort from holding the applied mass on their chest. This resulted in some participants terminating the exercise before a true strength assessment could be made. The crunches exercise is believed to be a poor choice when the goal involves loading the exercise close to maximum effort.

For the glute bridge exercise, one participant experienced discomfort from stabilizing the barbell on the hip bone, despite the use of padding material. This was believed to be the main reason for not increasing the load further. Using another exercise targeting the gluteus muscles, or the use of sufficient padding to limit discomfort could prove a better choice in the future.

6.2. Learning effect during strength training

To investigate the implication of familiarization of the exercises in the present study, one participant (p_{03}), with no prior experience in strength exercises, performed the field test once a week for four weeks. This was evaluated in order to estimate if simply performing the test once a week would alter the results significantly. Figure 20 shows the indexed changes in 1RM over the four weeks, with the first week being the baseline. The results shows large fluctuations between the four test sessions for most exercises, indicating that some neural adaptations occurred. Previous studies have shown a rapid increase in muscle strength for novice subjects in the first few sessions of strength exercise [25, 26], due to neural adaptations more than hypertrophy. This could imply that caution should be taken when including novice participants into strength exercise studies without a familiarization period before the actual test sessions. This is especially true with the aim of comparing the optimization results with the dynamometer results. Novice participants could have had a positive effect from participating in the field test prior to the dynamometer test, because of the familiarization acquired through the strength exercises.

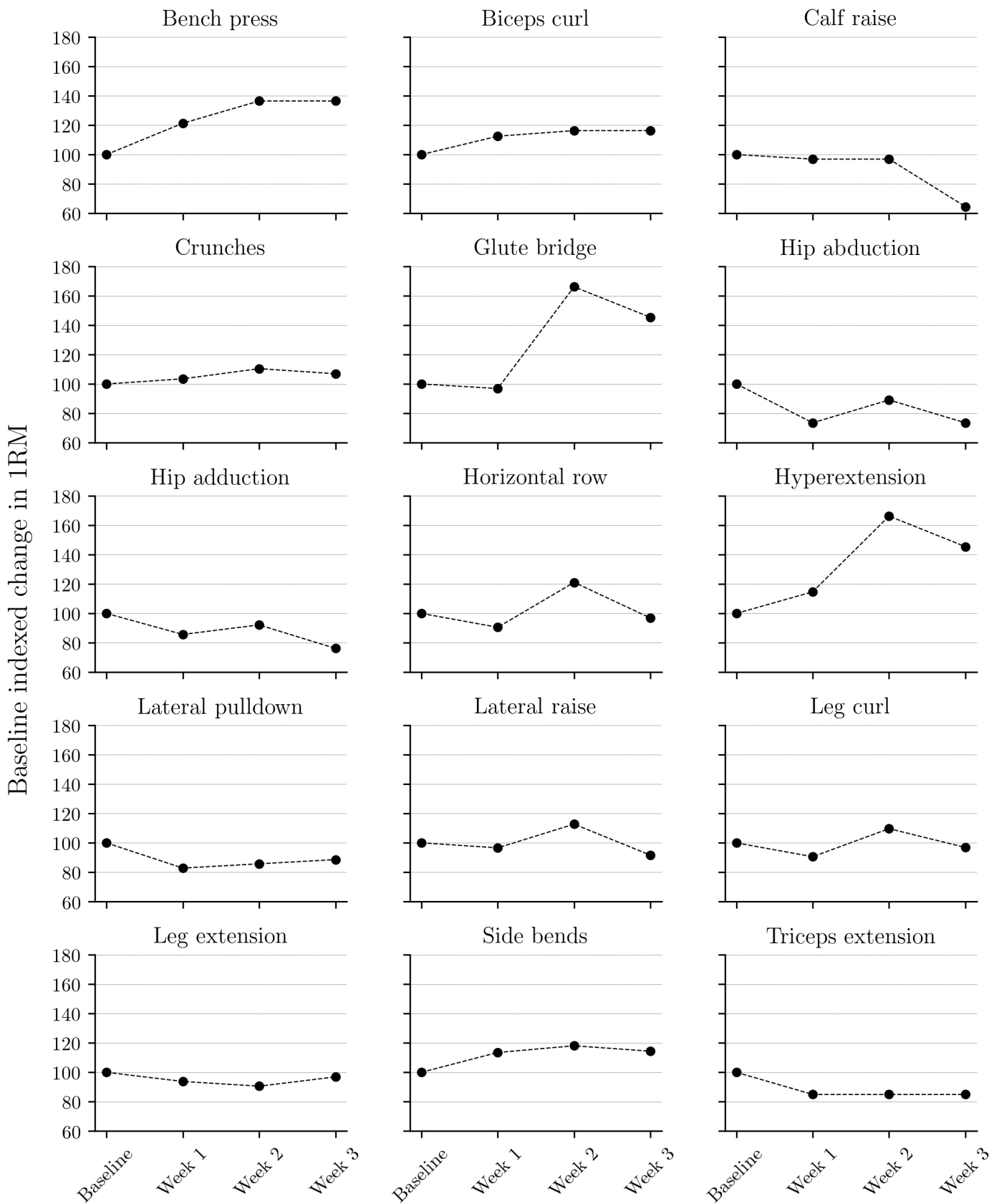


Figure 20: Baseline indexed change in one-repetition-maximum (1RM) compared to the first test session (baseline) for one participant (p_{03}), for each exercise, respectively.

References

- [1] J. Kompf and O. Arandjelović, “Understanding and overcoming the sticking point in resistance exercise,” *Sports Med.*, vol. 46, no. 6, pp. 751–762, 2016, ISSN: 0112-1642, 1179-2035. DOI: 10.1007/s40279-015-0460-2.
- [2] M. E. Lund, S. Tørholm, and M. Jung, *The AnyBody managed model repository (AMMR)*, Jun. 2018. DOI: 10.5281/zenodo.1287730.
- [3] V. Carbone, R. Fluit, P. Pellikaan, M. M. van der Krogt, D. Janssen, M. Damsgaard, L. Vigneron, T. Feilkas, H. F. J. M. Koopman, and N. Verdonschot, “TLEM 2.0 - a comprehensive musculoskeletal geometry dataset for subject-specific modeling of lower extremity,” en, *J. Biomech.*, vol. 48, no. 5, pp. 734–741, Mar. 2015, ISSN: 0021-9290, 1873-2380. DOI: 10.1016/j.jbiomech.2014.12.034.
- [4] M. de Zee, D. Falla, D. Farina, and J. Rasmussen, “A detailed rigid-body cervical spine model based on inverse dynamics,” *J. Biomech.*, vol. 40, S284, Jan. 2007, ISSN: 0021-9290. DOI: 10.1016/S0021-9290(07)70280-4.
- [5] M. de Zee, L. Hansen, C. Wong, J. Rasmussen, and E. B. Simonsen, “A generic detailed rigid-body lumbar spine model,” en, *J. Biomech.*, vol. 40, no. 6, pp. 1219–1227, 2007, ISSN: 0021-9290. DOI: 10.1016/j.jbiomech.2006.05.030.
- [6] H. E. J. Veeger, B. Yu, K. N. An, and R. H. Rozendal, “Parameters for modeling the upper extremity,” *J. Biomech.*, vol. 30, no. 6, pp. 647–652, 1997, ISSN: 0021-9290. DOI: 10.1016/S0021-9290(97)00011-0.
- [7] S. Skals, M. K. Jung, M. Damsgaard, and M. S. Andersen, “Prediction of ground reaction forces and moments during sports-related movements,” *Multibody Syst. Dyn.*, vol. 39, no. 3, pp. 175–195, Mar. 2017, ISSN: 1384-5640, 1573-272X. DOI: 10.1007/s11044-016-9537-4.
- [8] M. S. Andersen, M. Damsgaard, B. MacWilliams, and J. Rasmussen, “A computationally efficient optimisation-based method for parameter identification of kinematically determinate and over-determinate biomechanical systems,” en, *Comput. Methods Biomech. Biomed. Engin.*, vol. 13, no. 2, pp. 171–183, 2010, ISSN: 1025-5842, 1476-8259. DOI: 10.1080/10255840903067080.
- [9] A. Erdemir, S. McLean, W. Herzog, and A. J. Van den Bogert, “Model-based estimation of muscle forces exerted during movements,” *Clin. Biomech.*, vol. 22, no. 2, pp. 131–154, 2007, ISSN: 0268-0033. DOI: 10.1016/j.clinbiomech.2006.09.005.
- [10] J. Rasmussen, M. Damsgaard, and M. Voigt, “Muscle recruitment by the min/max criterion - a comparative numerical study,” *J. Biomech.*, vol. 34, no. 3, pp. 409–415, 2001, ISSN: 0021-9290. DOI: 10.1016/S0021-9290(00)00191-3.
- [11] J. Rasmussen, M. de Zee, M. Damsgaard, S. T. Christensen, C. Marek, and K. Siebertz, “A general method for scaling Musculo-Skeletal models,” in *2005 International Symposium on Computer Simulation in Biomechanics, Cleveland, Ohio, USA*, 2005, 2–2 pp.
- [12] D. A. Winter, *Biomechanics and Motor Control of Human Movement, 4th Edition*. Oct. 2009, ISBN: 9780470398180.
- [13] D. C. Frankenfield, W. A. Rowe, R. N. Cooney, J. S. Smith, and D. Becker, “Limits of body mass index to detect obesity and predict body composition,” *Nutrition*, vol. 17, no. 1, pp. 26–30, 2001, ISSN: 0899-9007. DOI: 10.1016/S0899-9007(00)00471-8.
- [14] C. C. Gordon, “1988 anthropometric survey of US army personnel: Methods and summary statistics,” *Technical Report Natick/TR-89/044*, 1989.
- [15] D. B. Hollander, R. R. Kraemer, M. W. Kilpatrick, Z. G. Ramadan, G. V. Reeves, M. Francois, E. P. Hebert, and J. L. Tryniecki, “Maximal eccentric and concentric strength discrepancies between young men and women for dynamic resistance exercise,” en, *J. Strength Cond. Res.*, vol. 21, no. 1, pp. 34–40, Feb. 2007, ISSN: 1064-8011. DOI: 10.1519/R-18725.1.
- [16] B. C. Elliott, G. J. Wilson, and G. K. Kerr, “A biomechanical analysis of the sticking region in the bench press,” *Med. Sci. Sports Exercise*, vol. 21, no. 4, 450??462, 1989, ISSN: 0195-9131. DOI: 10.1249/00005768-198908000-00018.
- [17] R. Van Den Tillaar, V. Andersen, and A. H. Saeterbakken, “The existence of a sticking region in free weight squats,” *J. Hum. Kinet.*, vol. 42, no. 1, pp. 63–71, 2014, ISSN: 1640-5544, 1899-7562. DOI: 10.2478/hukin-2014-0061.
- [18] J. Kompf and O. Arandjelović, “The sticking point in the bench press, the squat, and the deadlift: Similarities and differences, and their significance for research and practice,” *Sports Med.*, vol. 47, no. 4, pp. 631–640, 2017, ISSN: 0112-1642, 1179-2035. DOI: 10.1007/s40279-016-0615-9.
- [19] M. E. Lund, M. S. Andersen, and J. Rasmussen, *AnyPyTools*, Oct. 2018. DOI: 10.5281/zenodo.1474200.
- [20] T. Oliphant, *NumPy: A guide to NumPy*, USA: Trelgol Publishing, [Online; accessed ;today;], 2006-. [Online]. Available: <http://www.numpy.org/>.
- [21] W. McKinney, “Data structures for statistical computing in python,” in *Proceedings of the 9th Python in Science Conference*, S. van der Walt and J. Millman, Eds., 2010, pp. 51–56.
- [22] S. G. Johnson, *The NLOpt nonlinear-optimization package*, 2014.
- [23] M. Lund, J. Rasmussen, and M. Andersen, “Anypyttools: A python package for reproducible research with the anybody modeling system,” *Journal of Open Source Software*, vol. 4, p. 1108, Jan. 2019. DOI: 10.21105/joss.01108.
- [24] M. J. D. Powell, “The NEWUOA software for unconstrained optimization without derivatives,” in *Large-Scale Nonlinear Optimization*, G. Di Pillo and M. Roma, Eds., Boston, MA: Springer US, 2006, pp. 255–297, ISBN: 9780387300658. DOI: 10.1007/0-387-30065-1_16.
- [25] D. A. Gabriel, G. Kamen, and G. Frost, “Mechanisms and recommendations for training practices,” *Res. Sports Med.*, vol. 36, no. 2, pp. 133–149, 2006, ISSN: 1543-8627.
- [26] T. Moritani, “Neuromuscular adaptations during the acquisition of muscle strength, power and motor tasks,” en, *J. Biomech.*, vol. 26 Suppl 1, pp. 95–107, 1993, ISSN: 0021-9290.